공학석사학위논문

일군의 동적 논홀로노믹 기계시스템의 수동성기반 적응 및 강건 안정화 제어기법 연구

Adaptive and Robust Passivity-Based Stabilization of a Class of Nonholonomic Mechanical Systems

2016 년 8 월

서울대학교 대학원

기계항공공학부

Kent Yee Lui

일군의 동적 논홀로노믹 기계시스템의 수동성기반 적응 및 강건 안정화 제어기법 연구

Adaptive and Robust Passivity-Based Stabilization of a Class of Nonholonomic Mechanical Systems

지도교수 이 동 준

이 논문을 공학석사 학위논문으로 제출함

2016 년 4 월

서울대학교 대학원

기계항공공학부

Kent Yee Lui

Kent Yee Lui 의 공학석사 학위논문을 인준함

2016 년 6 월

위 원 장 이 경 수

부위원장 이 동 준

위 원 박 종 우

Abstract

Adaptive and Robust Passivity-Based Stabilization of a Class of Nonholonomic Mechanical Systems

Kent Yee Lui
Mechanical & Aerospace Engineering
The Graduate School
Seoul National University

We present novel passivity-based stabilization control frameworks for a class of nonholonomic mechanical systems with uncertain inertial parameters. Passive configuration decomposition is first applied to configuration-level decompose the system's Lagrange-D'Alembert dynamics into two separate systems. Each of these decomposed systems evolves on its respective configuration space and individually inherits Lagrangian structure and passivity from the original dynamics. Utilizing the nonlinearity and passivity of the decomposed dynamics, we then derive adaptive passivity-based time-varying control (APBVC) and robust passivity-based switching control (RPBSC) schemes, which adopt the concepts of adaptive control and sliding-mode control respectively to achieve stabilization for this certain class of nonholonomic mechanical systems. Both simulation and experimental results are provided to verify our proposed control frameworks.

Keywords: Nonholonomic constraints, uncertain inertial parameters, adaptive control, robust control
Student Number: *2014-22194*

Contents

List of Figures

Abbreviations

NMS	**N**onholonomic **M**echanical **S**ystem
WMR	**W**heeled **M**obile **R**obot
PBC	**P**assivity-**B**ased **C**ontrol
PBVC	**P**assivity-**B**ased Time-**V**arying **C**ontrol
APBVC	**A**daptive **P**assivity-**B**ased Time-**V**arying **C**ontrol
PBSC	**P**assivity-**B**ased **S**witching **C**ontrol
RPBSC	**R**obust **P**assivity-**B**ased **S**witching **C**ontrol

Symbols

$\mathcal{I}$	Inertial frame	
$\mathcal{B}$	Body-fixed frame rigidly attached to the WMR	
q ($\dot{q}$, $\ddot{q}$)	Configuration (velocity, acceleration) in $\{\mathcal{I}\}$	$\in \Re^n$
τ	Control	$\in \Re^n$
$M(q)$	Inertia matrix	$\in \Re^{n \times n}$
$C(q, \dot{q})$	Coriolis matrix	$\in \Re^{n \times n}$
$A(q)$	Nonholonomic constraint	$\in \Re^{p \times n}$

Chapter 1

Introduction

1.1 Motivation and Objectives

Robots have been developed to help human achieve various tasks, including but not limited to surveillance, assembly, military application etc. One of the common applications, i.e. logistic and material handling, has been benefited greatly from the capability of robots to carry payloads [1]. Notable examples for this would be the recent mobile robots by Amazon Robotics and Fetch Robotics. These systems utilize nonholonomic mobile robots to handle warehouse payloads, which are often unknown a priori and could be heavy and large. These would then introduce uncertainty to the inertial parameters of the robots, since there is no guarantee that the payloads will always be similar in masses and shapes. There could be

a considerably large additional mass to, or shift of the center of mass of the unloaded systems. A similar situation is applicable to healthcare applications as well. Human on average weigh as light as 30[kg] for an elementary school student, and as heavy as 70[kg] for a fully-grown adult. Such wide weight range naturally introduces large uncertainty to the electrical wheelchairs which are supposed to carry human with different weights.

To deal with inertial uncertainty under such situations, we propose adaptive and robust passivity-based controls in this thesis. Passivity-based control exploits the nonlinear dynamics of robotic systems, instead of attempting to completely cancel out and replace it by linear dynamics. This would then improve the robustness of controllers. Moreover, the storage function and skew-symmetry property of $\dot{M}(q) - 2C(q, \dot{q})$, where $M \in \Re^{n \times n}, C \in \Re^{n \times n}, q \in \Re^n$ are respectively the inertia matrix, Coriolis matrix, and the configuration with n being the degrees-of-freedom (DOFs), also substantially simplify the adaptive and robust control analysis for systems with uncertainties [2].

Passivity-based control framework has been extensively applied to many topics in robotics, such as under-actuated robots [3, 4], flexible manipulators [5, 6], manipulator motion control [7, 8], interaction control [9, 10], biped walking [11], teleoperation [12, 13], and so on. However, passivity-based control has yet to be rigorously attempted on the feedback control of nonholonomic mechanical systems, let alone the cases with the presence of uncertainties which necessitate adaptive and robust control frameworks. Moreover, most works regarding the

feedback control of nonholonomic mechanical systems involve only kinematic analysis. For more practically useful applications, dynamics control would be necessary due to its capability to achieve fast and smooth motion.

In this thesis, we propose novel passivity-based stabilization control frameworks for a class of nonholonomic mechanical systems with uncertain inertial parameters. We first exploit the symmetry structure of this class of nonholonomic mechanical systems and use passive configuration decomposition to configuration-level decompose the system's Lagrange-D'Alembert dynamics into two separate systems. Utilizing the nonlinearity and passivity of these decomposed dynamics, we then develop adaptive passivity-based time-varying control (APBVC) and robust passivity-based switching control (RPBSC) schemes for the dynamic feedback control of nonholonomic mechanical systems. To the best of our knowledge, our result is one of the first results on adaptive and robust passivity-based feedback control of the dynamics of nonholonomic mechanical systems with inertial uncertainty.

1.2 State of the Art

The majority of feedback control of nonholonomic mechanical systems are based on specific control forms (e.g., normal form, power form, chained form, etc.), that can be typically attained only by feedback linearization and state transformation (e.g., [14–22]). Some rare exceptions are [23–25]. Nonlinear dynamics is utilized

in some works [26–30], but only for open-loop control or controllability analysis of the nonholonomic mechanical systems. Adaptive and robust controls have also been applied to nonholonomic mechanical systems. However, these works are mostly kinematic instead of dynamics [14, 31], and/or utilize specific control forms [32–35]. Moreover, none of these are verified with real experiments. Sliding-mode control framework for nonholonomic wheeled mobile robots is experimentally verified in [36], where instead of passivity-based control, feedback linearization is utilized. This work also focuses on external noises instead of parameter uncertainties.

1.3 Contribution of this Work

In this thesis, we propose adaptive and robust stabilization control frameworks for a class of nonholonomic mechanical systems with uncertain inertial parameters. More specifically, we utilize passivity-based control to design feedback control for the dynamics of nonholonomic mechanical systems with symmetry structure. To the best of our knowledge, this work is one of the first results on the adaptive and robust passivity-based controls for the dynamics of nonholonomic mechanical systems.

To be more specific, we present adaptive passivity-based time-varying control (APBVC) and robust passivity-based switching control (RPBSC) schemes to achieve stabilization for a class of nonholonomic mechanical systems containing

inertial uncertainty, while exploiting the Lagrangian dynamics structure and passivity of the systems. This work is, in fact, an extension of [37], where the nominal counterparts of our control schemes: passivity-based time-varying control (PBVC) and passivity-based switching control (PBSC) schemes are proposed. In this extension work, we show that our proposed frameworks are robust against inertial uncertainty (e.g. parameters are hard to be estimated, payloads with unknown masses etc), even that of very high one. The adaptive and sliding-mode actions of our frameworks compensate for the uncertainty and allow us to achieve the desired stabilization effectively. We could then possibly utilize these control frameworks of nonholonomic mechanical systems on various practical applications such as logistics and transportation as mentioned in Sec. 1.1.

The rest of this thesis is organized as follows. The class of nonholonomic mechanical systems analyzed in this thesis is introduced in Ch. 2, along with passive configuration decomposition [37], which is utilized to decompose the dynamics of the aforementioned class of nonholonomic mechanical systems. Adaptive passivity-based time-varying control and robust passivity-based switching control are derived in Ch. 3 and Ch. 4 respectively. The simulation and experimental results are shown in Ch. 5. Finally, this thesis is concluded in Ch. 6.

Chapter 2

System Description

2.1 Nonholonomic Mechanical Systems with Symmetry Structure

The dynamics of nonholonomic mechanical systems is widely known to be consisting of 1) nonholonomic Pfaffian constraint:

$$A(q)\dot{q} = 0 \tag{2.1}$$

and 2) Lagrange-D'Alembert equation of motion:

$$M(q)\ddot{q} + C(q,\dot{q})\dot{q} + A^T(q)\lambda = \tau + f \tag{2.2}$$

where $q, \dot{q}, \tau, f \in \Re^n$ are the configuration, velocity, control, and external force, $M, C \in \Re^{n \times n}$ are the inertia and Coriolis matrices with $\dot{M} - 2C$ being skew-symmetric, $A(q) \in \Re^{p \times n}$ $(p \leq n)$ defines the nonholonomic constraint, and $A^T(q)\lambda$ is the constraint force, which magnitude is represented by the Lagrange multiplier $\lambda \in \Re^p$. We (locally) identify the system's configuration space $\mathcal{M}$ by $q \in \Re^n$ (i.e., $\mathcal{M} \approx \Re^n$). We also assume that the nonholonomic constraint (2.1) is smooth, regular (i.e. rank$A(q) = p$ for all q), and does not contain inertial uncertainty.

In this work, we consider a class of nonholonomic mechanical systems with the following properties for (2.1)-(2.2): 1) the configuration space $\mathcal{M}$ can be endowed with the product structure s.t.

$$\mathcal{M} = \mathcal{S} \times \mathcal{R}$$

with $q := [s; r]$, $s \in \Re^{n-m}$ and $r \in \Re^m$; 2) the inertia matrix is a function of only $r \in \mathcal{R}$, that is, $M(q) = M(r)$ and $C(q, \dot{q}) = C(r, \dot{q})$ for (2.2); and 3) the nonholonomic Pfaffian constraint (2.1) is a function of only $r \in \mathcal{R}$ and applies constraint only on $\mathcal{S}$, that is,

$$A(q)\dot{q} = \begin{bmatrix} A_s(r) & 0_{p \times m} \end{bmatrix} \dot{q} = A_s(r)\dot{s} = 0 \tag{2.3}$$

with $A_s(r) \in \Re^{p \times (n-m)}$ being full row-rank. This class of systems, though seemingly restricted, actually contains many practically important systems (e.g. mobile manipulator [38], beanie [39], vertical coin [40], differential-drive wheeled

mobile robot [41], etc).

These properties allow us to write the unconstrained distribution for (2.1)-(2.2) as:

$$\mathcal{D}(r) := \text{span} \begin{bmatrix} \mathcal{D}_s(r) & 0 \\ 0 & I_{m\times m} \end{bmatrix} \tag{2.4}$$

where $\mathcal{D}_s(r) \in \Re^{(n-m)\times(n-m-p)}$ defines the unconstrained distribution on $\mathcal{S}$ s.t. $A_s(r)\mathcal{D}_s(r) = 0$. Since we assume $A(q)$ to be regular and smooth, so are $\mathcal{D}$ and $\mathcal{D}_s$ with $\text{rank}[\mathcal{D}(r)] = n - p$ and $\text{rank}[\mathcal{D}_s(r)] = n - m - p$ $\forall r \in \mathcal{R}$ respectively.

2.2 Passive Configuration Decomposition

Following nonholonomic passive decomposition [23], we can decompose the dynamics (2.2) while also considering the nonholonomic constraint (2.1) and preserving the Lagrangian structure and passivity of (2.2) as follow.

Similar to the base variable [15, 42], we define $h(q) := r$ to represent the unconstrained $\dot{r}$-dynamics on $\mathcal{R}$. We also define the null-space of $\partial h/\partial q$ by $\Delta^\top \subset T_q\mathcal{M}$, and its orthogonal complement w.r.t. the M-metric by $\Delta^\perp \subset T_q\mathcal{M}$, where $T_q\mathcal{M} \approx \Re^n$ is the tangent space of $\mathcal{M}$ at q. The structure of $h(q) = r$ signifies that $\Delta^\top = \text{span}[I_{(n-m)\times(n-m)}; 0_{m\times(n-m)}]$, i.e., $\Delta^\top \approx T_s\mathcal{S} \approx \Re^{n-m}$. Since the nonholonomic constraint (2.3) only acts on $\mathcal{S}$, we can then find that

$\mathcal{D} \cap \Delta^{\top} = \text{span}[\mathcal{D}_s(r); 0_{m\times(n-m)}]$. The description above is better illustrated in Fig. 2.1.

Now, we can then write $\dot{q}$ s.t.,

$$\dot{q} = \begin{pmatrix} \dot{s} \\ \dot{r} \end{pmatrix} = \underbrace{\begin{bmatrix} \mathcal{D}_s(r) & \beta(r) \\ 0 & I_{m\times m} \end{bmatrix}}_{=:S(r)\in\Re^{n\times(n-p)}} \begin{pmatrix} \nu_s \\ \dot{r} \end{pmatrix} \tag{2.5}$$

where

$$\beta(r) := -\mathcal{D}_s(r)[\mathcal{D}_s^T(r)M_1(r)\mathcal{D}_s(r)]^{-1}\mathcal{D}_s^T(r)M_2(r) \tag{2.6}$$

enforces the M-orthogonality between $\text{span}[\mathcal{D}_s(r); 0] = \mathcal{D}\cap\Delta^{\top}$ and $\text{span}[\beta(r); I_{m\times m}] = \mathcal{D} \setminus [\mathcal{D} \cap \Delta^{\top}]$. In other words,

$$S^T M S = \begin{bmatrix} \mathcal{D}_s^T M_1 \mathcal{D}_s & 0 \\ 0 & \beta^T M_1 \beta + \beta^T M_2 + M_2^T \beta + M_3 \end{bmatrix}$$

with the inertia matrix $M(r)$ in (2.2) written as

$$M(r) =: \begin{bmatrix} M_1(r) & M_2(r) \\ M_2^T(r) & M_3(r) \end{bmatrix} \tag{2.7}$$

where $M_1 \in \Re^{(n-m)\times(n-m)}$, $M_2 \in \Re^{(n-m)\times m}$ and $M_3 \in \Re^{m\times m}$. The inverse term in $\beta(r)$ always exists since $M_1(r)$ is invertible and $\mathcal{D}_s(r)$ has a full column rank.

The full column rank of $\mathcal{D}_s(r)$ also allows us to always assume that $\mathcal{D}_s^T\mathcal{D}_s = I$.

Following [23], we can decompose the unconstrained distribution $\mathcal{D}$ of nonholonomic mechanical systems as below:

$$\mathcal{D} = (\mathcal{D} \cap \Delta^\top) \oplus (\mathcal{D} \cap \Delta^\perp) \oplus \mathcal{D}^c$$

where $\mathcal{D}^c$ is the *quotient distribution*, which is M-orthogonal with $\mathcal{D} \cap \Delta^\top$ and $\mathcal{D} \cap \Delta^\perp$. This quotient distribution is contained in $\mathcal{D}$ but neither exclusively in $\Delta^\top$ nor $\Delta^\perp$ since it contains components in both $\Delta^\top$ and $\Delta^\perp$. A system is strongly decomposable if $\mathcal{D}^c = \emptyset$, and weakly decomposable otherwise [23]. Generally, most nonholonomic mechanical systems are only weakly decomposable.

We can then decompose the Lagrange-D'Alembert dynamics (2.2) using (2.5) s.t.

$$H_s(r)\dot{\nu}_s + Q_s(r,\dot{q})\nu_s + Q_{sr}(r,\dot{q})\dot{r} = u_s + \delta_s \tag{2.8}$$

$$H_r(r)\ddot{r} + Q_r(r,\dot{q})\dot{r} + Q_{rs}(r,\dot{q})\nu_s = u_r + \delta_r \tag{2.9}$$

where (2.8) and (2.9) are the projected dynamics on $\mathcal{D} \cap \Delta^\top$ and $\mathcal{D} \setminus [\mathcal{D} \cap \Delta^\top]$ respectively, with their projected inertia given by $\text{diag}[H_s, H_r] := S^T M S$,

$$\begin{bmatrix} Q_s & Q_{sr} \\ Q_{rs} & Q_r \end{bmatrix} := S^T \left[M\dot{S} + CS \right] \tag{2.10}$$

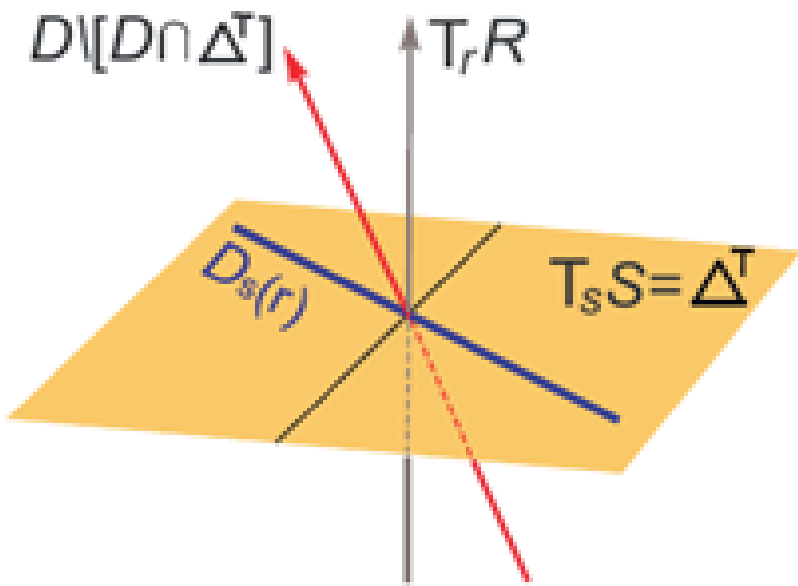

FIGURE 2.1: Illustration of $T_s\mathcal{S} \approx \Delta^\top$, $T_r\mathcal{R}$, $\mathcal{D}_s(r) \approx \mathcal{D} \cap \Delta^\top$ and $\mathcal{D} \setminus [\mathcal{D} \cap \Delta^\top]$. Note that $\Delta^\top$ is Euclidean orthogonal w.r.t. $T_r\mathcal{R}$, and M-orthogonal w.r.t. $\mathcal{D} \setminus [\mathcal{D} \cap \Delta^\top]$.

and

$$\begin{pmatrix} u_s \\ u_r \end{pmatrix} := S^T(r) \begin{pmatrix} \tau_s \\ \tau_r \end{pmatrix} = \begin{pmatrix} \mathcal{D}_s^T \tau_s \\ \beta^T(r)\tau_s + \tau_r \end{pmatrix} \tag{2.11}$$

are the projected controls with $\tau_s \in \Re^{n-m}$ and $\tau_r \in \Re^m$. The similar hold for $f_\star$ and $\delta_\star$ as well. The proposition below (also Prop. 1 in [37]) shows that the Lagrangian structure and passivity of the original system (2.1)-(2.2) are preserved in the decomposition (2.8)-(2.9), with the original kinetic energy and power also

decomposed into those of ν_s and $\dot{r}$ dynamics.

Proposition 1. Consider the nonholonomic mechanical system (2.1)-(2.2) with the properties as stated in Sec. 2.1. Then, we can decompose its dynamics (2.1)-(2.2) into (2.8)-(2.9), where

1. H_s and H_r are symmetric and positive-definite.
2. $\dot{H}_s - 2Q_s$ and $\dot{H}_r - 2Q_r$ are skew-symmetric.
3. $Q_{sr} = -Q_{rs}^T$.
4. Kinetic energy and power are decomposed s.t.

$$\kappa(t) = \frac{1}{2}\nu_s^T H_s \nu_s + \frac{1}{2}\dot{r}^T H_r \dot{r}, \quad \tau^T \dot{q} = u_s^T \nu_s + u_r^T \dot{r}$$

(similar also hold for f and δ), where $\kappa := \dot{q}^T M \dot{q}/2$.

Proof: See [23]. ∎

From (2.5), we can express $\dot{s}$ as

$$\dot{s} = \mathcal{D}_s(r)\nu_s + \beta(r)\dot{r} \tag{2.12}$$

where $\mathcal{D}_s(r)\nu_s$ is the *dynamic phase* and $\beta(r)\dot{r}$ is the *geometric phase* [42]. In general, $\mathcal{D} \setminus [\mathcal{D} \cap \Delta^\top]$ is not "aligned with" or "parallel to" $T_r\mathcal{R}$. Therefore,

motion along $\mathcal{D} \setminus [\mathcal{D} \cap \Delta^\top]$ will generate some artifact motion on $\mathcal{S}$ as given by $\beta(r)\dot{r}$.

However, as can be seen from Fig. 2.1, if $\beta(r) = 0$, we have $\mathcal{D} \setminus [\mathcal{D} \cap \Delta^\top] = \text{span}[0_{(n-m)\times m}; I_{m\times n}] \approx T_r\mathcal{R}$. This means that $\mathcal{D} \setminus [\mathcal{D} \cap \Delta^\top]$ is now aligned with $T_r\mathcal{R}$ and the geometric phase motion $\beta(r)\dot{r}$ on $\mathcal{S}$ disappears. We can then decompose the motion $q \in \mathcal{M}$ of the original nonholonomic mechanical system (2.1)-(2.2) into motion on $\mathcal{S}$, which evolves following the ν_s-dynamics (2.8) with $\dot{s} = \mathcal{D}_s(r)\nu_s$ and motion on $\mathcal{R}$ respecting the $\dot{r}$-dynamics (2.9).

The decomposition (2.8)-(2.9) with $\beta(r) = 0$ is defined as **passive configuration decomposition** into $\mathcal{S}$ and $\mathcal{R}$ [37]. This condition of $\beta(r) = 0$ is fulfilled if the Euclidean orthogonality and the M-metric orthogonality of $\mathcal{D} \setminus [\mathcal{D} \cap \Delta^\top]$ w.r.t. $\Delta^\top$ become the same, i.e. iff $M_2^T(r)\mathcal{D}_s(r) = 0$ for all r (see Lem. 1 of [37]).

2.3 Control Objective

In this thesis, we consider a stabilization control problem, which control objective is $q = (s; r) \to (s_d; r_d) =: q_d$, where s_d and r_d are desired constant set-points on $\mathcal{S}$ and $\mathcal{R}$ respectively. We assume that (u_s, u_r) in (2.11) can be arbitrary, i.e., the nonholonomic mechanical system (2.1)-(2.2) is fully-actuated in $\mathcal{D}$. In general, this is a necessary assumption to obtain control forms or kinematic representations similar to the majority of literature on the feedback control of nonholonomic mechanical systems [14–22].

Since both ν_s-dynamics and $\dot{r}$-dynamics individually evolve on configuration spaces $\mathcal{S}$ and $\mathcal{R}$ respectively, we may use standard configuration-based control techniques (e.g., trajectory tracking, potential field, etc), including passivity-based control on $\mathcal{S}$ and $\mathcal{R}$ independently. This is possible since both ν_s-dynamics and $\dot{r}$-dynamics retain the Lagrangian structure and passivity from (2.2) as mentioned above.

Unlike $s \to s_d$, we can easily achieve $r \to r_d$ since the $\dot{r}$-dynamics (2.9) on $\mathcal{R}$ is not constrained by the nonholonomic Pfaffian constraint (2.3). However, although the motion in $\mathcal{S}$ is restricted by the nonholonomic constraint (2.3), we can still achieve $s \to s_d$ by utilizing the Lagrangian structure and passivity of the ν_s-dynamics (2.8), i.e. by applying the potential function technique and Lyapunov-like analysis based on passivity. For this, let us define a non-negative smooth navigation potential on $\mathcal{S}$:

$$\varphi_s : \mathcal{S} \to \Re$$

s.t. 1) $\varphi_s(s) \geq 0$ where $\varphi_s(s) = 0$ iff $s = s_d$; 2) $\partial\varphi_s/\partial s(s) := [\partial\varphi_s/\partial s_1, ..., \partial\varphi_s/\partial s_{n-m}]$ $= 0$ iff $s = s_d$; and 3) for any $l \geq 0$, the level set

$$\mathcal{L}_l := \{s \in \mathcal{S} \mid \varphi_s(s) \leq l\} \tag{2.13}$$

is a compact set containing $s = s_d$ and $\mathcal{L}_{l_1} \subseteq \mathcal{L}_{l_2}$ if $0 \leq l_1 \leq l_2$. Note that φ_s is designed as if the configuration space $\mathcal{S}$ is unconstrained by the nonholonomic

constraint. This allows us to adopt potential functions designed for unconstrained robots [43].

In the next Ch. 3 and 4, we design and analyze novel adaptive and robust passivity-based stabilization control frameworks for nonholonomic mechanical systems with inertial uncertainty. In fact, the stabilization control frameworks proposed are the robustified versions of the control frameworks proposed in [37].

Chapter 3

Passivity-Based Time-Varying Control

3.1 Nominal Passivity-Based Time-Varying Control

With the navigation potential φ_s in Sec. 2.3, the nominal control u_s in (2.8) is designed in [37] to be

$$u_s = Q_{sr}(r, \dot{q})\dot{r} - b_s\nu_s - \mathcal{D}_s^T(r)\left[\frac{\partial\varphi_s(s)}{\partial s}\right]^T - \delta_s \tag{3.1}$$

where $b_s \in \Re^{(n-m-p)\times(n-m-p)}$ is a positive-definite symmetric damping gain, $Q_{sr}\dot{r}$ is the decoupling control, and $\partial\varphi_s/\partial s \in \Re^{1\times(n-m-p)}$ is the one-form of

$\varphi_s(s)$. This results in the closed-loop ν_s-dynamics (2.8) s.t.

$$H_s(r)\dot{\nu}_s + Q_s(r,\dot{q})\nu_s + b_s\nu_s + \mathcal{D}_s^T(r)\left[\frac{\partial\varphi_s(s)}{\partial s}\right]^T = 0. \tag{3.2}$$

Utilizing Prop. 1 and Lyapunov analysis, we obtain the following energetics, with $\beta(r) = 0$:

$$V_s(T) - V_s(0) = -\int_0^T ||\nu_s||_{b_s}^2 dt, \quad \forall T \geq 0 \tag{3.3}$$

where $V_s(t) := \kappa_s(t) + \varphi_s(t)$ is the chosen Lyapunov function, $\kappa_s := \nu_s^T H_s \nu_s/2$ the kinetic energy of ν_s-dynamics (2.8), and $||\nu_s||_{b_s}^2 := \nu_s^T b_s \nu_s$ the b_s-dissipation. Note that the closed-loop ν_s-dynamics (3.2) and the energetics (3.3) are the same as those of usual robot systems. This observation then leads to the following proposition (also Prop. 2 in [37]).

Proposition 2. Consider the ν_s-dynamics (2.8) with u_s in (3.1) and $\beta(r) = 0$. Suppose further that: 1) partial derivatives of $M(r)$ w.r.t. r of any order are bounded; 2) partial derivatives of $\varphi_s(s)$ w.r.t. s of any order are bounded if $\varphi_s(s)$ is bounded; and 3) $\dot{r}, \ddot{r} \in \mathcal{L}_\infty$. Then, $\nu_s \to 0$ and

$$\mathcal{D}_s^T(r)\left[\frac{\partial\varphi_s(s)}{\partial s}\right]^T \to 0. \tag{3.4}$$

Proof: See [37]. ∎

Note that the unconstrained $\dot{r}$-dynamics can be controlled to track any desired trajectory $r_o(t) \in \Re^m$ by using

$$u_r := Q_{rs}\nu_s + H_r\ddot{r}_o + Q_r\dot{r}_o - k_d(\dot{r} - \dot{r}_o) - k_p(r - r_o) - \delta_r \tag{3.5}$$

where $Q_{rs}\nu_s$ is the decoupling control, and $k_d, k_p \in \Re^{m\times m}$ are the control gains. Since Prop. 2 holds despite $r(t)$ keeps varying, we can drive r so that the null space of $\mathcal{D}_s^T(r)$ keeps "rotating". Then, (3.4) will necessarily enforce $\partial\varphi_s(s)/\partial s \to 0$ similar to the persistency of excitation for parameter convergence of adaptive control [44]. This also means that we enforce $s \to s_d$ due to the properties of φ_s. Such strategy leads to the nominal passivity-based time-varying control proposed in [37], which is restated in Th. 1 below (also Th. 2 in [37]).

Theorem 1. Consider the ν_s-dynamics (2.8) with u_s (3.1) and $\beta(r) = 0$. Assume the same as in Prop. 2. Suppose further that, controlling (2.9), we drive $r(t)$ in such a way that the following persistency of excitation condition holds: $\forall t' \geq 0$, $\exists$ a bounded $\Delta t \geq 0$ s.t.,

$$\mathcal{D}_s^T(r(t))\left[\frac{\partial\varphi_s(s)}{\partial s}\right]^T = 0 \;\; \forall t \in [t', t' + \Delta t) \;\; \text{iff} \;\; \frac{\partial\varphi_s(s)}{\partial s} = 0. \tag{3.6}$$

Then, $\nu_s \to 0$ and $s \to s_d$.

3.2 Adaptive Passivity-Based Time-Varying Control

We now extend the results in Sec. 3.1 by including adaptive action to deal with inertial uncertainties, i.e. mass, moment of inertia etc, which are often difficult to be estimated. On the other hand, kinematic uncertainties are in general relatively easy to be estimated and assumed to be known. Therefore, here, we assume H and Q to be uncertain, and terms such as $\nu_s, \dot{r}, \delta_s, \delta_r$ are certain, since the reduction matrix (2.5) is free from inertial parameters and purely kinematic.

Similar to (3.1), we design the control u_s in (2.8) s.t

$$u_s = \hat{Q}_{sr}(r, \dot{q})\dot{r} - b_s\nu_s - \mathcal{D}_s^T(r)\left[\frac{\partial \varphi_s(s)}{\partial s}\right]^T - \delta_s \tag{3.7}$$

where the terms are defined the same as in (3.1). In this thesis, we denote the estimated term of $\star$ by $\hat{\star}$. In this case, only $\hat{Q}_{sr}(r, \dot{q})$ contains inertial parameters. From (2.10), we now linear parameterize this uncertain term $\hat{Q}_{sr}(r, \dot{q})$ as follows [2]:

$$\hat{Q}_{sr}(r, \dot{q})\dot{r} = \mathcal{D}_s^T(r)\hat{C}_2(r, \dot{q})\dot{r} = \mathcal{D}_s^T(r)Y_{sr}(r, \dot{q})\hat{\Theta} \tag{3.8}$$

where $Y_{sr} \in \Re^{(n-p-m)\times l}$ is the linear parameterization matrix of $\hat{C}_2(r, \dot{q})\dot{r}$ with $\hat{\Theta} \in \Re^l$ being the vector of uncertain inertial parameters.

With (3.8) incorporated into (3.7), the closed-loop ν_s-dynamics (2.8) on $\mathcal{S}$ then becomes

$$H_s\dot{\nu}_s + Q_s\nu_s + \mathcal{D}_s^T Y_{sr}\tilde{\Theta} + b_s\nu_s + \mathcal{D}_s^T\left[\frac{\partial\varphi_s(s)}{\partial s}\right]^T = 0 \tag{3.9}$$

where $\tilde{\Theta} := \Theta - \hat{\Theta}$. Let us now define a Lyapunov function $V(t) := \kappa_s(t) + \varphi_s(t) + \frac{1}{2\gamma}\tilde{\Theta}^T\tilde{\Theta}$, where $\gamma > 0$, and again, $\kappa_s := \nu_s^T H_s\nu_s/2$ the kinetic energy of ν_s-dynamics (2.8). We also define

$$\dot{\hat{\Theta}} = -\gamma Y_{sr}^T(r,\dot{q})\mathcal{D}_s(r)\nu_s \tag{3.10}$$

to be our adaptation law for the estimated parameter vector $\hat{\Theta}$.

Furthermore, from Prop. 1 with (2.12) and (3.9), we can derive

$$\begin{aligned}\frac{d\kappa_s}{dt} &= -||\nu_s||_{b_s}^2 - \frac{\partial\varphi_s}{\partial s}\mathcal{D}_s\nu_s - \nu_s^T\mathcal{D}_s^T Y_{sr}\tilde{\Theta} \\ &= -||\nu_s||_{b_s}^2 - \frac{d\varphi_s(s)}{dt} + \frac{\partial\varphi_s(s)}{\partial s}\beta(r)\dot{r} - \nu_s^T\mathcal{D}_s^T Y_{sr}\tilde{\Theta}\end{aligned}$$

where $d\varphi_s/dt = [\partial\varphi_s/\partial s]\dot{s}$. Utilizing the fact that $\beta(r) = 0$, we can then find dV/dt to be:

$$\begin{aligned}\frac{dV}{dt} &= \frac{d\kappa_s}{dt} + \frac{d\varphi_s(s)}{dt} + \frac{1}{\gamma}\tilde{\Theta}^T\dot{\tilde{\Theta}} \\ &= -||\nu_s||_{b_s}^2 - \nu_s^T\mathcal{D}_s^T Y_{sr}\tilde{\Theta} - \frac{1}{\gamma}\tilde{\Theta}^T\dot{\hat{\Theta}} \\ &= -||\nu_s||_{b_s}^2\end{aligned}$$

with the adaptation law $\dot{\hat{\Theta}}$ defined in (3.10).

Integrating this, we further have:

$$V(T) - V(0) = -\int_0^T ||\nu_s||_{b_s}^2 dt, \qquad \forall T \geq 0 \tag{3.11}$$

Hence, similar to Sec. 3.1, the energetics (3.11) again become the same as those of common robotic systems. Note that this is possible due to the energy conservation properties of passivity-based control. Based on this observation, we can then formulate the following proposition.

Proposition 3. Consider the ν_s-dynamics (2.8) with u_s (3.7) and $\beta(r) = 0$. Suppose that: 1) partial derivatives of $M(r)$ w.r.t. r of any order are bounded; 2) partial derivatives of $\varphi_s(s)$ w.r.t. s of any order are bounded if $\varphi_s(s)$ is bounded; and 3) $\dot{r}, \ddot{r} \in \mathcal{L}_\infty$. Then, $\nu_s \to 0$ and

$$\mathcal{D}_s^T(r) \left[Y_{sr}(r, \dot{q})\tilde{\Theta} + \left[\tfrac{\partial \varphi_s(s)}{\partial s} \right]^T \right] \to 0. \tag{3.12}$$

Proof: Given $\beta(r) = 0$, we have $\nu_s \in \mathcal{L}_\infty \cap \mathcal{L}_2$ from (3.11). This means $\dot{q} \in \mathcal{L}_\infty$ with $\dot{r} \in \mathcal{L}_\infty$ assumed. We also know that $\varphi_s(t) \leq V(t) \leq V(0)\ \forall t \geq 0$. Therefore, $\partial\varphi_s/\partial s \in \mathcal{L}_\infty$. Also, note that $Q(r, \dot{q})$ (hence, $Y_{sr}(r, \dot{q})$) is linear w.r.t. $\partial M_{ij}/\partial q_k$ and $\dot{q}$, with $\mathcal{D}(r)$ being smooth. Following (3.11), we can also see that $\tilde{\Theta} \in \mathcal{L}_\infty$ since $V(t) := \kappa_s(t) + \varphi_s(t) + \frac{1}{2\gamma}\tilde{\Theta}^T\tilde{\Theta}$. Then, from (3.9), we have $\dot{\nu}_s \in \mathcal{L}_\infty$. Also, $\ddot{q} \in \mathcal{L}_\infty$ with $\ddot{r} \in \mathcal{L}_\infty$. Then, from Barbalat's lemma [44], $\nu_s \to 0$. We can also verify that $\ddot{\nu}_s \in \mathcal{L}_\infty$ by differentiating (3.9). Again, from Barbalat's lemma, $\dot{\nu}_s \to 0$.

We then complete the proof by applying $(\nu_s, \dot{\nu}_s) \to 0$ to (3.9). ■

Since Prop. 3 also holds despite $r(t)$ keeps varying, we can again drive r so that the null space of $\mathcal{D}_s^T(r)$ keeps "rotating" similar to the persistency of excitation for parameter convergence [44]. Then, (3.12) will necessarily enforce $Y_{sr}(r, \dot{q})\tilde{\Theta} + [\partial\varphi_s(s)/\partial s]^T \to 0$. In general, $Y_{sr}(r, \dot{q})\tilde{\Theta}$ and $[\partial\varphi_s(s)/\partial s]^T$ will not be in the same direction. Furthermore, since $r(t)$ keeps varying, even if $Y_{sr}(r, \dot{q})\tilde{\Theta}$ and $[\partial\varphi_s(s)/\partial s]^T$ are in the same direction for a moment, they generally will not be so all the time. Hence, if we excite r richly enough, we may achieve both $Y_{sr}(r, \dot{q})\tilde{\Theta} \to 0$ and $[\partial\varphi_s(s)/\partial s]^T \to 0$ (see Ch. 5). This is possible since the r-dynamics (2.9) is fully-actuated. We may choose any decent $r_o(t)$ to achieve this persistency of excitation condition, with the only restriction being the structure of $\mathcal{D}_s(r)$. Note that $[\partial\varphi_s(s)/\partial s]^T \to 0$ means $s \to s_d$ from the structure of $\varphi_s(s)$. We may even further achieve $\tilde{\Theta} \to 0$ with sufficiently rich r. The strategy above leads to the **adaptive passivity-based time-varying control**, which is formalized in the following Th. 2.

Theorem 2. Consider the ν_s-dynamics (2.8) with u_s (3.7) and $\beta(r) = 0$. Assume the same as in Prop. 3. Suppose further that, controlling (2.9), we drive $r(t)$ in such a way that the following persistency of excitation condition holds: $\forall t' \geq 0$,

$\exists$ a bounded $\Delta t \geq 0$ s.t.,

$$\mathcal{D}_s^T(r(t)) \left[Y_{sr}(r, \dot{q})\tilde{\Theta} + \left[\tfrac{\partial \varphi_s(s)}{\partial s}\right]^T \right] = 0 \quad \forall t \in [t', t' + \Delta t)$$
$$\text{iff} \quad Y_{sr}(r, \dot{q})\tilde{\Theta} = 0 \text{ and } \left[\tfrac{\partial \varphi_s(s)}{\partial s}\right]^T = 0. \tag{3.13}$$

Then, $\nu_s \to 0$ and $s \to s_d$.

In order to drive $r(t)$ s.t. $r(t) \to r_o(t)$, we can design the control u_r in (2.9) similar to (3.5) s.t.

$$u_r = \hat{Q}_{rs}\nu_s + \hat{H}_r\ddot{r}_o + \hat{Q}_r\dot{r}_o - k_d(\dot{r} - \dot{r}_o) - k_p(r - r_o) - \delta_r$$

where the terms are defined as in (3.5). However, since the role of u_r in the time-varying control framework is technically to drive r richly enough to achieve the persistent excitation (3.13) of Th. 2, we can instead adopt a simpler PD-control as below

$$u_r = -k_d(\dot{r} - \dot{r}_o) - k_p(r - r_o) - \delta_r \tag{3.14}$$

with high-enough gains and no uncertain terms, because of the Lagrangian structure and passivity of the r-dynamics (2.9). Therefore, the inertial uncertainty only affects the ν_s-dynamics (2.8) in $\mathcal{S}$ due to $\hat{Q}_{sr}\dot{r}$ for our adaptive passivity-based time-varying control framework with u_s (3.7) and PD-control u_r (3.14) above.

Now, let us denote the set of $r(t)$ constituting the persistency of excitation condition (3.13) by $\mathcal{R}_o \subset \mathcal{R}$. If there exists $t' \geq t$ for any $t \geq 0$ s.t. $r_d(t') \in \mathcal{R}_o$, we can achieve our control objective of $q = (s, r) \to q_d = (s_d, r_d)$. Otherwise, we can instead replace $r_o(t)$ in (3.14) with the desired constant set-point r_d when ν_s and $\varphi_s(s)$ are small enough, thereby achieving $r \to r_d$ while keeping $||s - s_d||$ arbitrarily small, where $||\star||^2 := \star^T \star$. This strategy can be applied as a practical stopping threshold, i.e., once $V = \kappa_s + \varphi_s + \frac{1}{2\gamma}\tilde{\Theta}^T\tilde{\Theta}$ decreases until a pre-defined threshold (user-defined performance specification), we can then replace r_o in (3.14) by r_d despite some error in φ_s, similar to the practical stabilization [22].

To be more precise, let us assume that $\kappa_s(t') \leq \epsilon_1$, $\varphi_s(t') \leq \epsilon_2$ and $\frac{1}{2\gamma}\tilde{\Theta}(t')^T\tilde{\Theta}(t') \leq \epsilon_3$ at time $t' \geq 0$ with small $\epsilon_1, \epsilon_2, \epsilon_3 > 0$. Since $\kappa_s \geq 0$, from (3.11), we have $\varphi_s(t) \leq \epsilon_1 + \epsilon_2 + \epsilon_3$ for all $t \geq t'$, regardless of the motion of r. Hence, switching $r_o(t)$ in (3.14) to r_d when $\kappa_s(t) \leq \epsilon_1$, $\varphi_s(t) \leq \epsilon_2$ and $\frac{1}{2\gamma}\tilde{\Theta}(t)^T\tilde{\Theta}(t) \leq \epsilon_3$ enforces exact stabilization of $r \to r_d$, and also ensures $||s - s_d||$ being small as given by $\varphi_s \leq \epsilon_1 + \epsilon_2 + \epsilon_3$, with $\epsilon_1, \epsilon_2, \epsilon_3 > 0$ being small. Note that since $\nu_s(t) \to 0$ is always guaranteed from Prop. 3, we may simply wait long enough for $\nu_s(t)$ to converge to zero, i.e. $\epsilon_1 \approx 0$ for smaller $||s - s_d||$.

Chapter 4

Passivity-Based Switching Control

4.1 Nominal Passivity-Based Switching Control

Let us now stabilize r to a constant $r_\sigma \in \mathcal{R}$, where σ is to embed a switching sequence, using the proportional-derivative control to the r-dynamics (2.9) on $\mathcal{R}$ as below:

$$u_r := Q_{rs}\nu_s - k_d\dot{r} - k_p(r - r_\sigma) - \delta_r \tag{4.1}$$

where $k_p, k_d \in \Re^{m\times m}$ are the control gains. From Prop. 2, s will then converge to the switching manifold $\mathcal{G}_\sigma \subset \mathcal{S}$ defined as

$$\mathcal{G}_\sigma := \{s \in \mathcal{S} \mid \mathcal{D}_s^T(r_\sigma)\left[\frac{\partial \varphi_s(s)}{\partial s}\right]^T = 0\}. \tag{4.2}$$

We then further trigger the switching s.t. $\sigma \Leftarrow 2$ with $\mathcal{G}_1 \neq \mathcal{G}_2$ once s stabilizes on the switching manifold $\mathcal{G}_1$ with $\sigma = 1$ and small ν_s. We denote the instance when this i^{th} switching occurs as $t_i \geq 0$, and the time when s stabilizes to $\mathcal{G}_2$ with small ν_s as $t_{i+1} > t_i$. We may again trigger another switching at t_{i+1} with $\sigma \Leftarrow 1$.

Then, from (3.3), the energetics during the interval $I_i := [t_i, t_{i+1})$ will be:

$$\begin{aligned}\varphi_s(t_{i+1}) - \varphi_s(t_i) &= \kappa_s(t_i) - \kappa_s(t_{i+1}) - \int_{t_i}^{t_{i+1}} ||\nu_s||_{b_s} dt \\ &\leq \kappa_s(t_i) - \int_{t_i}^{t_{i+1}} ||\nu_s||_{b_s}^2 dt \end{aligned} \tag{4.3}$$

with $\kappa_s(t_{i+1}) \geq 0$. We can therefore guarantee the strict decrease of φ_s if the last line of (4.3) is strictly negative. The navigation potential $\varphi_s(t)$ will then eventually approach 0, i.e. $s \to s_d$, if we switch between manifolds repetitively. In order for the last line of (4.3) to be strictly negative, the b_s-dissipation in (4.3) will need to absorb $\kappa_s(t_i)$ totally. The following lemma (also Lem. 2 in [37]) shows that this is possible if: 1) we trigger switching at t_i when $\kappa_s(t_i)$ is small enough, i.e. $\nu_s(t_i) \leq \epsilon_v(D)$ since $\kappa_s := \nu_s^T H_s \nu_s/2$; and 2) the system traverses a far enough distance D on $\mathcal{S}$ between t_i and t_{i+1}.

Lemma 1. Suppose $||s(t_{i+1}) - s(t_i)|| \geq D > 0$. Then, there always exists $\epsilon_v(D) > 0$ s.t., if $||\nu_s(t_i)|| \leq \epsilon_v(D)$,

$$\int_{t_i}^{t_{i+1}} ||\nu_s||_{b_v}^2 dt > \kappa_s(t_i).$$

where $|| \star ||^2 := \star^T \star$.

Proof: See [37]. ∎

Lem. 1 leads to the nominal passivity-based switching control proposed in [37], which is restated in Th. 3 below (also Th. 3 in [37]). Note that instead of only two switching manifolds, we may use p_s switching manifolds $\mathcal{G}_{\sigma(i)}$ with $\sigma(i) \in \{1, 2, ..., p_s\}$, where $\sigma(i)$ defines the switching index for $I_{i-1} = [t_{i-1}, t_i)$ $(i = 1, 2, ...)$. This switching index is constant during I_{i-1}. We also define the "strip" $\bar{\mathcal{G}}_{\sigma(i)}$ with the thickness of $\delta_m > 0$ s.t. $\bar{\mathcal{G}}_{\sigma(i)} := \{s \in \mathcal{S} \mid \text{dist}(s, \mathcal{G}_{\sigma(i)}) \leq \delta_m\}$ as shown in Fig. 4.1, where $\text{dist}(x, y)$ is the minimum Euclidean distance between x and y.

Theorem 3. Consider (2.8)-(2.9) with u_s (3.1) and u_r (4.1). Assume the same as Prop. 2. Suppose that, given $\delta_o > 0$, we can find $\varphi_s(s)$, $\delta_m > 0$ and $D > 0$ s.t., for any $\sigma \in \{1, 2, .., p_s\}$ and $s \in \mathcal{S}$, if $s \in \bar{\mathcal{G}}_\sigma$, yet, $s \notin \mathcal{L}_{\delta_o}$ (see (2.13)), $\exists$ a non-empty set $W(s, \sigma) \subset \{1, 2, ...p_s\}$ s.t., the following switching manifold

separation condition is granted:

$$\text{dist}(s, \bar{\mathcal{G}}_{\sigma'}) \geq D, \quad \forall \sigma' \in W(s, j) \tag{4.4}$$

where $\bar{\mathcal{G}}_\star$ is the strip of $\mathcal{G}_\star$ with δ_m-thickness. Trigger the switching at $t =: t_i > t_{i-1}$ with $\sigma(i+1) \in W(s(t), \sigma(i))$, if 1) $s(t) \notin \mathcal{L}_{\delta_o}$; 2) $\text{dist}(s(t), \mathcal{G}_{\sigma(i)}) \leq \delta_m$; and 3) $||\nu_s(t)|| \leq \epsilon_v(D)$, where $\epsilon_v(D)$ is defined in Lem. 1. Then, $\lim_{t\to\infty} s(t) \in \mathcal{L}_{\delta_o}$.

Proof: See [37]. ∎

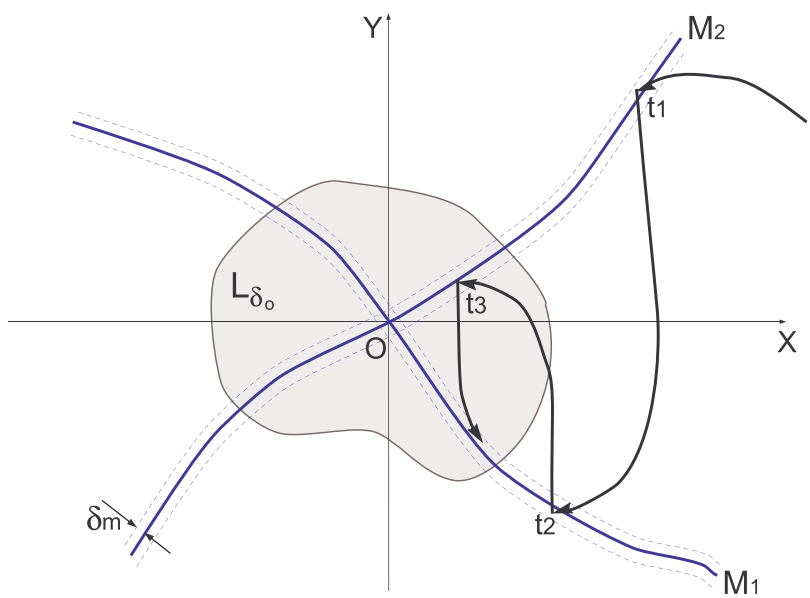

FIGURE 4.1: Illustration of passivity-based switching on $\Re^2$, with two switching manifolds $\mathcal{G}_1$, $\mathcal{G}_2$; strips $\bar{\mathcal{G}}_1$, $\bar{\mathcal{G}}_2$ with δ_m thickness; and the level set $\mathcal{L}_{\delta_o}$.

4.2 Robust Passivity-Based Switching Control

We now extend the results in Sec. 4.1 by including sliding-mode action as below to deal with inertial uncertainties, i.e. mass, moment of inertia etc, which are often difficult to be estimated. Similar to Sec. 3.2, we assume that only inertial uncertainty exists, which again means that H and Q are uncertain, while the kinematic terms such as $\nu_s, \dot{r}, \delta_s, \delta_r$ have no uncertainty.

We shall note that the decoupling term $Q_{sr}\dot{r}$ in u_s of our passivity-based switching and time-varying control frameworks is needed to prevent the energy jumping in the spring k_p due to switching of r_σ for switching control, and the energy pumping from driving $r_o(t)$ for time-varying control. Without $Q_{sr}\dot{r}$, the energy may flow back to the ν_s-dynamics and invalidate the energetics (4.15) below (for switching control) and (3.11) (for time-varying control) on $\mathcal{S}$. Then, the strict decrease of φ_s will not be always guaranteed.

With the existence of uncertainties, $\tilde{Q}_{sr}\dot{r}$, i.e. imperfect decoupling due to the error of parameter estimation is typically unavoidable. However, since the ν_s-dynamics inherits passivity property with the uncertainty satisfying the matching condition [2], we can reject "energy leak" from $\tilde{Q}_{sr}\dot{r}$ back into the ν_s-dynamics with the following control:

$$u_s = \hat{Q}_{sr}(r,\dot{q})\dot{r} - b_s\nu_s - \mathcal{D}_s^T(r)\left[\frac{\partial\varphi_s(s)}{\partial s}\right]^T - \delta_s - \eta||\dot{r}||\mathrm{sgn}(\nu_s) \tag{4.5}$$

where the last term is a sliding-mode like term with sufficiently large $\eta > 0$ and sgn($\star$) is a signum function. Note that since $Q_{sr} = -Q_{rs}^T$, we only need to estimate one uncertain term in our control framework, e.g. estimate Q_{sr} in (4.5) to also obtain Q_{rs} in (4.9).

With (4.5), the closed-loop ν_s-dynamics (2.8) on $\mathcal{S}$ then becomes

$$H_s\dot{\nu}_s + Q_s\nu_s + \tilde{Q}_{sr}\dot{r} + b_s\nu_s + \mathcal{D}_s^T\left[\frac{\partial\varphi_s}{\partial s}\right]^T + \eta||\dot{r}||\text{sgn}(\nu_s) = 0 \tag{4.6}$$

Let us now define a Lyapunov function $V(t) := \kappa_s(t) + \varphi_s(t)$. From Prop. 1 with (2.12) and (4.6), we can derive

$$\begin{aligned}\frac{d\kappa_s}{dt} &= -||\nu_s||_{b_s}^2 - \frac{\partial\varphi_s}{\partial s}\mathcal{D}_s\nu_s - \nu_s^T\tilde{Q}_{sr}\dot{r} - \nu_s^T\eta||\dot{r}||\text{sgn}(\nu_s)\\ &= -||\nu_s||_{b_s}^2 - \frac{d\varphi_s(s)}{dt} + \frac{\partial\varphi_s(s)}{\partial s}\beta(r)\dot{r}\\ &\quad - \nu_s^T\tilde{Q}_{sr}\dot{r} - \nu_s^T\eta||\dot{r}||\text{sgn}(\nu_s)\end{aligned}$$

where $\kappa_s := \nu_s^T H_s\nu_s/2$, $||\nu_s||_{b_s}^2 := \nu_s^T b_s\nu_s$, and $d\varphi_s/dt = [\partial\varphi_s/\partial s]\dot{s}$. Utilizing the fact that $\beta(r) = 0$, we can then find dV/dt to be:

$$\begin{aligned}\frac{dV}{dt} &= \frac{d\kappa_s}{dt} + \frac{d\varphi_s(s)}{dt}\\ &= -||\nu_s||_{b_s}^2 - \nu_s^T\tilde{Q}_{sr}\dot{r} - \nu_s^T\eta||\dot{r}||\text{sgn}(\nu_s)\\ &\leq -||\nu_s||_{b_s}^2\end{aligned} \tag{4.7}$$

Here, the last line is granted if $\eta \geq \bar{\sigma}[\tilde{Q}_{sr}(r, \dot{q})]$, that is, the last term of u_s (4.5) is able to absorb all energy leak to the ν_s-dynamics from the imperfect decoupling $\tilde{Q}_{sr}\dot{r}$. Note the second line of (4.7). We can see that the term $\nu_s^T \eta ||\dot{r}|| \text{sgn}(\nu_s)$ is linear w.r.t. both ν_s and $\dot{r}$ since η is purely a constant, while the term $\nu_s^T \tilde{Q}_{sr}\dot{r}$ is quadratic w.r.t. at least one of ν_s and $\dot{r}$ due to $\tilde{Q}_{sr}(r, \dot{q})$ being a function of $\dot{q}$. Hence, we can always find η s.t. $\eta \geq \bar{\sigma}[\tilde{Q}_{sr}(r, \dot{q})]$ to ensure the last line of (4.7), especially since $Q(r, \dot{q})$ is assumed to be bounded.

Integrating (4.7), we further have:

$$V(T) - V(0) \leq -\int_0^T ||\nu_s||_{b_s}^2 dt, \quad \forall T \geq 0 \tag{4.8}$$

Hence, if $\beta(r) = 0$, the energetics (4.8) again become the same as those of common robotic systems. Similar to the case of adaptive passivity-based time-varying control, this is possible due to the energy conservation properties of passivity-based control.

Now, similar to Sec. 4.1, we stabilize r to a constant $r_\sigma \in \mathcal{R}$, where σ is to embed a switching sequence. Due to the existence of uncertain terms, this shall be achieved by using the standard sliding-mode control [2] to the $\dot{r}$-dynamics (2.9) as follows:

$$\begin{aligned} u_r &= \hat{Q}_{rs}\nu_s - k_d\dot{r} - k_p(r - r_\sigma) - \delta_r \\ &= Y_{rs}(\hat{\Theta} + \delta u_r) - k_d\dot{r} - k_p(r - r_\sigma) - \delta_r \end{aligned} \tag{4.9}$$

where $k_p, k_d \in \Re^{m\times m}$ are the control gains, $Y_{rs}\hat{\Theta}$ is the linear parameterization of $\hat{Q}_{rs}\nu_s$ with $\hat{\Theta}$ being the nominal parameter vector, and δu_r is the additional control term to compensate for the uncertainty. Following the typical approach of sliding-mode control, we can design δu_r to be

$$\delta u_r = \begin{cases} -\rho\frac{Y_{rs}^T\dot{r}}{||Y_{rs}^T\dot{r}||} & \text{if } ||Y_{rs}^T\dot{r}|| \neq 0 \\ 0 & \text{if } ||Y_{rs}^T\dot{r}|| = 0 \end{cases} \tag{4.10}$$

where ρ is the nonnegative constant upper bound of the uncertainty $||\Theta - \hat{\Theta}||$, i.e. $||\Theta - \hat{\Theta}|| \leq \rho$. This additional control δu_r is however discontinuous on the subspace defined by $||Y_{rs}^T\dot{r}|| = 0$, and may cause chattering where the control switches rapidly between the values in (4.10). Therefore, in practice, we may implement a continuous approximation to this discontinuous control to reduce such chattering as below:

$$\delta u_r = \begin{cases} -\rho\frac{Y_{rs}^T\dot{r}}{||Y_{rs}^T\dot{r}||} & \text{if } ||Y_{rs}^T\dot{r}|| > \epsilon \\ -\rho\frac{Y_{rs}^T\dot{r}}{\epsilon} & \text{if } ||Y_{rs}^T\dot{r}|| \leq \epsilon \end{cases} \tag{4.11}$$

where ϵ is chosen to be only as large as necessary to eliminate chattering. Let us denote S_δ as the smallest level set of Lyapunov function V containing $B(\delta)$, which is the ball of radius δ where δ is proportional to ϵ [2]. We also denote B_r as the smallest ball containing S_δ. Hence, in practice, the convergence of r is only ultimately bounded w.r.t. B_r due to the uncertainty. With ϵ chosen to be only as large as necessary, we can still sufficiently guarantee $r \to r_\sigma$ (see Ch. 5). In

fact, even without uncertainty, $r \to r_\sigma$ could take infinitely long time.

In contrast to Sec. 4.1, since the closed-loop ν_s-dynamics (4.6) is not smooth due to the signum function in (4.5), we cannot ensure the convergence of s to the switching manifold $\mathcal{G}_\sigma \subset \mathcal{S}$ defined by

$$\mathcal{G}_\sigma := \{s \in \mathcal{S} \mid \mathcal{D}_s^T(r_\sigma) \left[\frac{\partial \varphi_s(s)}{\partial s}\right]^T = 0\}. \tag{4.12}$$

However, note that the term $\tilde{Q}_{sr}\dot{r}$ can produce energy leak only if $\dot{r} \neq 0$. Hence, we may first control $r(t) \to r_\sigma$ in finite-time with (4.9). Once $\dot{r} \approx 0$, we then replace the discontinuous $\text{sgn}(\nu_s)$ in (4.5) with smooth $\text{sat}(\nu_s)$ as follows:

$$u_s = \hat{Q}_{sr}(r, \dot{q})\dot{r} - b_s\nu_s - \mathcal{D}_s^T(r) \left[\frac{\partial \varphi_s(s)}{\partial s}\right]^T - \delta_s - \eta||\dot{r}||\text{sat}(\nu_s) \tag{4.13}$$

With the closed-loop ν_s-dynamics now being smooth, we can ensure the convergence of s to $\mathcal{G}_\sigma$ (4.12). Note that if $\dot{r} = 0$, the closed-loop ν_s-dynamics (4.6) would naturally be smooth. This control strategy is formalized in the following proposition.

Proposition 4. Consider the ν_s-dynamics (2.8) with u_s in (4.5) (or (4.13) if $\dot{r} \approx 0$ after $r(t) \to r_\sigma$) and $\beta(r) = 0$. Suppose further that: 1) partial derivatives of $M(r)$ w.r.t. r of any order are bounded; 2) partial derivatives of $\varphi_s(s)$ w.r.t. s of any order are bounded if $\varphi_s(s)$ is bounded; 3) $\dot{r}, \ddot{r} \in \mathcal{L}_\infty$; 4) $M(r)$ is smooth;

and 5) $\dot{q}(0)$ is bounded with (4.8). Then, $\nu_s \to 0$ and

$$\mathcal{D}_s^T(r_\sigma)\left[\frac{\partial \varphi_s(s)}{\partial s}\right]^T \to 0. \tag{4.14}$$

Proof: First, with $\beta(r) = 0$, from (4.8), we have $\nu_s \in \mathcal{L}_\infty \cap \mathcal{L}_2$. This also means $\dot{q} \in \mathcal{L}_\infty$ with $\dot{r} \in \mathcal{L}_\infty$. Also, $\varphi_s(t) \leq V(t) \leq V(0)\ \forall t \geq 0$, thus, $\partial\varphi_s/\partial s \in \mathcal{L}_\infty$. Then, from (4.6) with the assumptions made above and the fact that $Q(r, \dot{q})$ is linear w.r.t. $\partial M_{ij}/\partial q_k$ and $\dot{q}$ (with $\mathcal{D}(r)$ being also smooth), we have $\dot{\nu}_s \in \mathcal{L}_\infty$ (and also $\ddot{q} \in \mathcal{L}_\infty$ with $\ddot{r} \in \mathcal{L}_\infty$). Then, from Barbalat's lemma [44], $\nu_s \to 0$. However, since the closed-loop ν_s-dynamics (4.6) is not smooth due to the signum function in (4.5), we cannot apply Barbalat's lemma as in Prop. 2 to show the convergence of (4.14). In order for us to apply Barbalat's lemma, we replace the discontinuous $\mathrm{sgn}(\nu_s)$ in (4.5) with smooth $\mathrm{sat}(\nu_s)$ as in (4.13) once $\dot{r} \approx 0$ after $r(t) \to r_\sigma$ in finite-time with the control strategy as mentioned above. Now, differentiating (4.6) with smooth $\mathrm{sat}(\nu_s)$ and the above assumptions, we can show that $\ddot{\nu}_s \in \mathcal{L}_\infty$. So, from Barbalat's lemma, $\dot{\nu}_s \to 0$. Applying $(\nu_s, \dot{\nu}_s) \to 0$ and $(r, \dot{r}) \to (r_\sigma, 0)$ to (4.6) shows the convergence of (4.14) and completes the proof. ■

From Prop. 4, s will then converge to the switching manifold (4.12). Let us suppose that once s stabilizes on the switching manifold $\mathcal{G}_1$ with $\sigma = 1$ and small ν_s, we then further trigger the switching s.t. $\sigma \Leftarrow 2$ with $\mathcal{G}_1 \neq \mathcal{G}_2$. We denote the instance when this i^{th} switching occurs as $t_i \geq 0$, and the time when

s stabilizes to $\mathcal{G}_2$ with small ν_s as $t_{i+1} > t_i$. We may again trigger another switching at t_{i+1} with $\sigma \Leftarrow 1$. Note that for each switching, we control $\mathcal{R}$ with (4.9) and $\mathcal{S}$ with (4.5); and once $\dot{r} \approx 0$, we use (4.13) instead of (4.5) to ensure the convergence to the switching manifold.

Then, from (4.8), the energetics during the interval $I_i := [t_i, t_{i+1})$ will be:

$$\begin{aligned}\varphi_s(t_{i+1}) - \varphi_s(t_i) &\leq \kappa_s(t_i) - \kappa_s(t_{i+1}) - \int_{t_i}^{t_{i+1}} ||\nu_s||_{b_s}^2 dt \\ &\leq \kappa_s(t_i) - \int_{t_i}^{t_{i+1}} ||\nu_s||_{b_s}^2 dt \end{aligned} \tag{4.15}$$

with $\kappa_s(t_{i+1}) \geq 0$. We can therefore guarantee the strict decrease of φ_s if the last line of (4.15) is strictly negative. The navigation potential $\varphi_s(t)$ will then eventually approach 0, i.e. $s \to s_d$, if we switch between manifolds repetitively. Similar to Sec. 4.1, in order for the last line of (4.15) to be strictly negative, the b_s-dissipation in (4.15) will need to absorb $\kappa_s(t_i)$ totally, which is possible if: 1) we trigger switching at t_i when $\kappa_s(t_i)$ is small enough, i.e. $\nu_s(t_i) \leq \epsilon_v(D)$ since $\kappa_s := \nu_s^T H_s \nu_s/2$; and 2) the system traverses a far enough distance D on $\mathcal{S}$ between t_i and t_{i+1}. In other words, even with uncertainty, our control framework here still behaves similarly to Lem. 1 and Th. 3 of the nominal passivity-based switching control. This is because we preserve the energetics (4.8) despite the uncertainty by exploiting the passivity of the systems. The strategy above leads to the **robust passivity-based switching control**, which is formalized in Th. 4 below. Again, we may use more than two switching manifolds, i.e. p_s switching

manifolds $\mathcal{G}_{\sigma(i)}$ with $\sigma(i) \in \{1, 2, ..., p_s\}$, where $\sigma(i)$ defines the switching index for $I_{i-1} = [t_{i-1}, t_i)$ $(i = 1, 2, ...)$.

Theorem 4. Consider (2.8)-(2.9) with u_s (4.5) (or (4.13)) and u_r (4.9). Assume the same as Prop. 4. Suppose that, given $\delta_o > 0$, we can find $\varphi_s(s)$, $\delta_m > 0$ and $D > 0$ s.t., for any $\sigma \in \{1, 2, .., p_s\}$ and $s \in \mathcal{S}$, if $s \in \bar{\mathcal{G}}_\sigma$, yet, $s \notin \mathcal{L}_{\delta_o}$ (see (2.13)), $\exists$ a non-empty set $W(s, \sigma) \subset \{1, 2, ...p_s\}$ s.t., the following switching manifold separation condition is granted:

$$\text{dist}(s, \bar{\mathcal{G}}_{\sigma'}) \geq D, \quad \forall \sigma' \in W(s, j) \tag{4.16}$$

where $\bar{\mathcal{G}}_\star$ is the strip of $\mathcal{G}_\star$ with δ_m-thickness. Trigger the switching at $t =: t_i > t_{i-1}$ with $\sigma(i+1) \in W(s(t), \sigma(i))$, if 1) $s(t) \notin \mathcal{L}_{\delta_o}$; 2) $\text{dist}(s(t), \mathcal{G}_{\sigma(i)}) \leq \delta_m$; and 3) $||\nu_s(t)|| \leq \epsilon_v(D)$, where $\epsilon_v(D)$ is defined in Lem. 1. Then, $\lim_{t\to\infty} s(t) \in \mathcal{L}_{\delta_o}$.

Proof: Recall that the closed-loop ν_s-dynamics (4.6) is not smooth due to the signum function in (4.5). With the control strategy mentioned above, i.e. replacing the discontinuous $\text{sgn}(\nu_s)$ in (4.5) with smooth $\text{sat}(\nu_s)$ as in (4.13) once $\dot{r} \approx 0$ after $r(t) \to r_\sigma$ in finite-time, we ensure the convergence of s to $\mathcal{G}_\sigma$ (4.12). Hence, we can now then follow the similar approach in [37] for the proof of Th. 4. ■

Similar to Sec. 3.2, if there exists $r_d \in \{r_1, r_2, ..., r_{p_s}\}$, we can enforce the separation condition (4.16) with $\delta_o = 0$, i.e., $\mathcal{L}_{\delta_o} = s_d \in \mathcal{S}$, to achieve our control objective of $q = (s, r) \to q_d = (s_d, r_d)$. Otherwise, if $r_d \notin \{r_1, r_2, ..., r_{p_s}\}$, we can simply trigger another switching with $r_\sigma \Leftarrow r_d$ in (4.9) once s stabilizes to $\mathcal{L}_{\delta_o}$

with small enough $||\nu_s||$. This allows us to achieve $r \to r_d$ while keeping $||s - s_d||$ small, instead of the asymptotic stabilization $q \to q_d$, which is more of a theoretical interest. Instead of $q = q_d$, a small enough $||q - q_d||$ would be sufficient in practice, since to achieve $q = q_d$ typically takes infinitely-long time.

To be more precise, denoting the last switching time by $\bar{t}$, we can find from (4.15) that

$$\varphi_s(t) \leq \varphi_s(\bar{t}) + \kappa_s(\bar{t})$$

for all $t \geq \bar{t}$. Therefore, despite the last switching $r_\sigma \Leftarrow r_d$, $\varphi_s(t)$, hence $||s - s_d||$ will remain small if $||\nu_s(\bar{t})||$ is small, e.g., $\kappa_s = \nu_s^T H_s \nu_s / 2 \leq \epsilon_1$. In other words, $\varphi_s(t) \leq \delta_o + \epsilon_1$, $\forall t \geq \bar{t}$, i.e. practical stabilization [22]. From Prop. 4, the switching conditions 2) and 3) in Th. 4 can be achieved by waiting long enough between switchings. Hence, we can reduce ϵ_1 to be very small by waiting long enough for each switching, thereby reducing $||s - s_d||$ during the final switching.

Chapter 5

Simulation and Experiment

5.1 Simulation

Using our control frameworks, we stabilize the formation of multiple wheeled mobile robots (WMRs) as below. Specifically, we stabilize N differential-drive WMRs' relative Cartesian positions to desired values without specifying the location of each of them, i.e., position consensus [45]. Note that our control frameworks are applicable to not only WMRs, but also every nonholonomic mechanical system with the properties mentioned in Sec. 2.1.

The configuration of the i^{th} WMR, as shown in Fig. 5.1, is given by $q_i = [x_i; y_i; \theta_i]$, where (x_i, y_i) is the Cartesian position of the geometric center and θ_i is the yaw angle relative to the inertial x-axis. These N WMRs may each have non-uniform

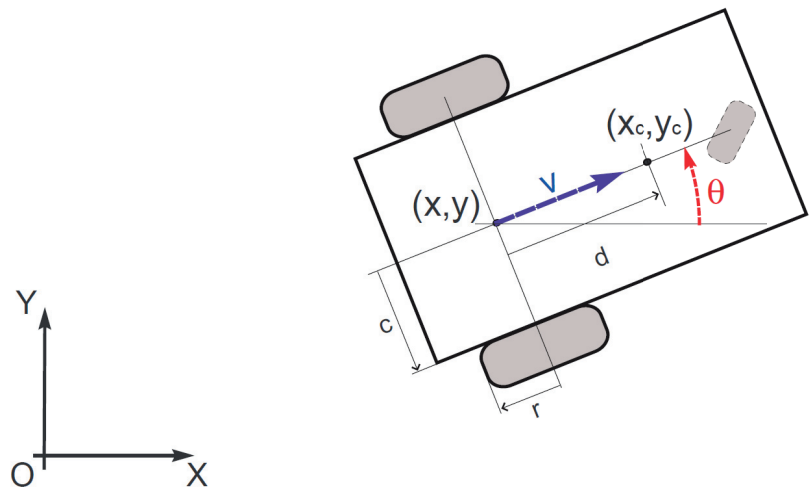

FIGURE 5.1: Differential-drive wheeled mobile robot (WMR) with inertial frame.

mass $m_i > 0$, moment of inertia $I_i > 0$ about the geometric center (x_i, y_i), and distance $d_i > 0$ between (x_i, y_i) and (x_{ci}, y_{ci}), where (x_{ci}, y_{ci}) is the center of mass. The Lagrangian of each WMR can then be written as

$$L_i = \frac{1}{2}\dot{q}_i^T \underbrace{\begin{bmatrix} m_i & 0 & -m_i d_i \,\mathrm{s}\,\theta_i \\ 0 & m_i & m_i d_i \,\mathrm{c}\,\theta_i \\ -m_i d_i \,\mathrm{s}\,\theta_i & m_i d_i \,\mathrm{c}\,\theta_i & I_i \end{bmatrix}}_{=:M_i(\theta_i)\in\Re^{3\times 3}} \dot{q}_i \tag{5.1}$$

and its no-slip nonholonomic constraint as

$$A_i(\theta_i)\dot{q}_i = \begin{bmatrix} \mathrm{s}\,\theta_i & -\mathrm{c}\,\theta_i & 0 \end{bmatrix} \dot{q}_i = 0$$

with the unconstrained distribution $\mathcal{D}_i(\theta_i)$ given by

$$\mathcal{D}_i(\theta_i) = \text{span} \begin{bmatrix} \text{c}\,\theta_i & 0 \\ \text{s}\,\theta_i & 0 \\ 0 & 1 \end{bmatrix} \tag{5.2}$$

where $\text{c}\,\theta_i = \cos\theta_i$ and $\text{s}\,\theta_i = \sin\theta_i$. Also, the Coriolis matrix is given by

$$C_i(\theta_i, \dot{\theta}_i) := \begin{bmatrix} 0 & 0 & -m_i d_i \dot{\theta}_i \,\text{c}\,\theta_i \\ 0 & 0 & -m_i d_i \dot{\theta}_i \,\text{s}\,\theta_i \\ 0 & 0 & 0 \end{bmatrix}$$

with $\dot{M}_i - 2C_i$ being skew-symmetric.

The product configuration of the N WMRs will then be $q := [s; r] \in \Re^{3N}$ with $s := [x_1; y_1; x_2; y_2; ...x_N; y_N] \in \Re^{2N}$ and $r := [\theta_1; \theta_2; ...\theta_N] \in \Re^N$. The product Lagrangian can then be written as $L := \frac{1}{2}\dot{q}^T M(r)\dot{q}$, with $M(r) \in \Re^{3N\times 3N}$ partitioned as in (2.7) with

$$M_{12}(r) = \text{diag}[M_1^{12}(\theta_1), M_2^{12}(\theta_2), ..., M_N^{12}(\theta_N)] \in \Re^{2N\times N}$$

where $M_i^{12}(\theta_i) := [-m_i d_i \,\text{s}\,\theta_i; m_i d_i \,\text{c}\,\theta_i] \in \Re^2$. We can also find the product unconstrained distribution $\mathcal{D}_s(r)$ (2.5) from (5.2) s.t.

$$\mathcal{D}_s(r) = \text{diag}[\mathcal{D}_{1s}(\theta_1), \mathcal{D}_{2s}(\theta_2), ..., \mathcal{D}_{Ns}(\theta_N)] \in \Re^{2N\times N}$$

where $\mathcal{D}_{is}(\theta_i) := [\mathrm{c}\,\theta_i; \mathrm{s}\,\theta_i] \in \Re^2$. Note the fact that

$$M_{12}^T(r)\mathcal{D}_s(r) = 0,$$

which means that the N WMRs are passive configuration decomposable with $\beta(r) = 0$. Note also that the product $\dot{M} - 2C$ is skew-symmetric.

We can also find $M_i\dot{S}_i + C_iS_i$ to be

$$M_i\dot{S}_i + C_iS_i := \begin{bmatrix} -m_i\dot{\theta}_i\,\mathrm{s}\,\theta_i & -m_id_i\dot{\theta}_i\,\mathrm{c}\,\theta_i \\ m_i\dot{\theta}_i\,\mathrm{c}\,\theta_i & -m_id_i\dot{\theta}_i\,\mathrm{s}\,\theta_i \\ m_id_i\dot{\theta}_i & 0 \end{bmatrix}$$

In order to linear parameterize as in (3.8), we would need C_{2i}, which is the top right block of $M_i\dot{S}_i + C_iS_i$ with the same size of $\mathcal{D}_{is}(\theta_i)$, i.e.

$$C_{2i} := \begin{bmatrix} -m_id_i\dot{\theta}_i\,\mathrm{c}\,\theta_i \\ -m_id_i\dot{\theta}_i\,\mathrm{s}\,\theta_i \end{bmatrix}$$

Now, we can compute the linear parameterization of $\hat{C}_{2i}\dot{r}_i$ for the i^{th} WMR as in (3.8):

$$\hat{C}_{2i}\dot{r}_i = \begin{bmatrix} -\hat{m}_id_i\dot{\theta}_i\,\mathrm{c}\,\theta_i \\ -\hat{m}_id_i\dot{\theta}_i\,\mathrm{s}\,\theta_i \end{bmatrix}\dot{r}_i = \begin{bmatrix} -\dot{\theta}_i^{\,2}\,\mathrm{c}\,\theta_i \\ -\dot{\theta}_i^{\,2}\,\mathrm{s}\,\theta_i \end{bmatrix}\hat{m}_id_i = Y_{sr_i}\hat{\Theta}_i$$

where $Y_{sr_i} = [-\dot{\theta}_i^2 \, \mathrm{c}\, \theta_i; -\dot{\theta}_i^2 \, \mathrm{s}\, \theta_i]$ and $\hat{\Theta}_i = \hat{m}_i d_i$. Following this, we can further compute the product linear parameterization of $\hat{C}_2(r, \dot{q})\dot{r}$ s.t.

$$Y_{sr} = \mathrm{diag}[Y_{sr_1}, Y_{sr_2}, ..., Y_{sr_N}] \in \Re^{2N \times N}$$

$$\hat{\Theta} = [\hat{\Theta}_1; \hat{\Theta}_2; ...\hat{\Theta}_N] \in \Re^N$$

Similarly, we can also compute Y_{rs} for (4.9), with product Q_{rs} given as:

$$Q_{rs} = \mathrm{diag}[m_1 d_1 \dot{\theta}_1, m_2 d_2 \dot{\theta}_2, ..., m_N d_N \dot{\theta}_N] \in \Re^{N \times N}$$

Linear parameterizing $Q_{rs}\nu_s$, we obtain Y_{rs} s.t.

$$Y_{rs} = \mathrm{diag}[Y_{rs_1}, Y_{rs_2}, ..., Y_{rs_N}] \in \Re^{N \times N}$$

where $Y_{rs_i} = \nu_{si}\dot{\theta}_i$.

We are now ready to define our navigation potential $\varphi_s(s)$ on $\mathcal{S} \approx \Re^{2N}$ to be:

$$\varphi_s(s) := \frac{1}{2} k_s (s - o_d)^T [\mathsf{L} \otimes I_{2\times 2}](s - o_d) \tag{5.3}$$

where $k_s > 0$ is the gain and $\otimes$ is the Kronecker product. $\mathsf{L} \in \Re^{N \times N}$ is the Laplacian matrix [45] of graph $\mathsf{G}(\mathsf{V}, \mathsf{E})$, which is assumed to be undirected and connected. The node set V symbolizes N WMRs and the edge set E contains the φ_s-potential links among the N nodes. We also define $o_d := [o_d^1; o_d^2; ...o_d^N] \in \Re^{2N}$

with $o_d^i - o_d^j$ specifying the desired Cartesian position offset between the i^{th} and the j^{th} WMRs. With the definitions above, $[\mathsf{L} \otimes I_{2\times 2}](s - o_d) \to 0$ means that $s - o_d \to 1_N \otimes c$ for an arbitrary $c \in \Re^2$. Hence, instead of stabilizing to fixed desired positions, the WMRs achieve the desired formation shape with an offset vector $c \in \Re^2$, i.e., E(2) symmetry.

We also define the control u_r (3.14) with $r_o = \theta_o(t) \cdot 1_N$ and u_r (4.9) with $r_\sigma = \theta_\sigma \cdot 1_N$, where $1_N = [1; 1; ...1] \in \Re^N$. The term $[\partial\varphi_s(s)/\partial s]^T$ of condition (3.12) in Prop. 3 and condition (4.14) in Prop. 4 can then be written as

$$k_s \begin{bmatrix} \mathrm{c}\,\theta & \mathrm{s}\,\theta & 0 & 0 & \cdots & 0 & 0 \\ 0 & 0 & \mathrm{c}\,\theta & \mathrm{s}\,\theta & \ddots & 0 & 0 \\ \vdots & \vdots & \ddots & \ddots & \ddots & \vdots & \vdots \\ 0 & 0 & 0 & 0 & \cdots & \mathrm{c}\,\theta & \mathrm{s}\,\theta \end{bmatrix} [\mathsf{L} \otimes I_{2\times 2}](s - o_d) \to 0$$

where $\theta := \theta_1 = \theta_2 = ...\theta_N$ with $\theta(t) = \theta_o(t)$ for the time-varying control or $\theta := \theta_\sigma$ for the switching control. Due to $I_{2\times 2}$, the term $\mathsf{L} \otimes I_{2\times 2}$ is diagonal, hence allowing us to define the relation above in a simpler expression s.t.,

$$\mathsf{L}(x - o_{dx})\,\mathrm{c}\,\theta + \mathsf{L}(y - o_{dy})\,\mathrm{s}\,\theta \to 0 \tag{5.4}$$

where $o_{dx} := [o_{dx}^1; o_{dx}^2; ...o_{dx}^N] \in \Re^N$ and $o_{dy} := [o_{dy}^1; o_{dy}^2; ...o_{dy}^N] \in \Re^N$ with $o_d^i := [o_{dx}^i; o_{dy}^i] \in \Re^2$. Therefore, the relation (5.4) will enforce $\mathsf{L}(x - o_{dx}) \to 0$ *and* $\mathsf{L}(y - o_{dy}) \to 0$, hence achieving $[\mathsf{L} \otimes I_{2\times 2}](s - o_d) \to 0$, i.e. the desired formation.

We perform simulations for four WMRs with the parameters $(m_1, I_1, d_1) = (6.7, 0.1, 0.1)$ for WMR 1, $(m_2, I_2, d_2) = (3.4, 0.4, 0.25)$ for WMR 2, $(m_3, I_3, d_3) = (3.4, 0.075, 0.12)$ for WMR 3, and $(m_4, I_4, d_4) = (4.2, 0.2, 0.075)$ for WMR 4. We also choose $k_s = 500$ for time-varying control and $k_s = 200$ for switching control, with the stopping criteria chosen to be $\varphi_s \leq 1 \times 10^{-5}$ and $\varphi_s \leq 2 \times 10^{-5}$ respectively. Here, we investigate two cases: 1) low inertial uncertainty, i.e. 15-30%; and 2) high inertial uncertainty, i.e. 70-85%. The simulation results are shown in Fig. 5.2 to 5.5 for passivity-based time-varying control (PBVC), Fig. 5.6 to 5.9 for adaptive passivity-based time-varying control (APBVC), Fig. 5.10 to 5.13 for passivity-based switching control (PBSC), and lastly Fig. 5.14 to 5.17 for robust passivity-based switching control (RPBSC).

For the cases of PBVC/APBVC (or PBSC/RPBSC respectively), we control r s.t. it increases linearly with time (or switches between two constant values) until the formation error is less than the stopping criteria chosen. From Fig. 5.2 and 5.10, we can see that with low inertial uncertainty, PBVC and PBSC are still able to stabilize the formation to a certain extent, despite the fact that the formation is not a perfect square as desired. In fact, the formation error does not decrease below a certain steady-state error due to the uncertainty, which could not be compensated without adaptive or sliding-mode actions. This steady-state error is larger if the inertial uncertainty is higher, i.e. the estimated parameter values deviate more from the true parameter values. This can be observed from Fig. 5.4 and 5.12 that the formation distorts much more for the cases with high inertial uncertainty. Nevertheless, we can still claim that the nominal counterparts of our

passivity-based control frameworks are robust particularly against low inertial uncertainty. Similar phenomenon can also be seen by comparing Fig. 5.3, 5.11 (low inertial uncertainty) with Fig. 5.5, 5.13 (high inertial uncertainty). We can see that the WMRs' x-positions oscillate w.r.t. the desired set-points, but not being able to converge to them. This oscillating behavior is even stronger for the cases with high inertial uncertainty. Note also that since the formation error does not decrease below our desired stopping criteria, r continues to increase linearly with time (or to switch between two constant values).

On the other hand, from Fig. 5.6 to 5.9 for APBVC and Fig. 5.14 to 5.17 for RPBSC, we can see that the formation stabilizes to a perfect square for both low and high inertial uncertainties. Instead of oscillating w.r.t. the desired set-points, the WMRs' x-positions converge shortly after about 17[sec] for APBVC and 15[sec] for RPBSC even with high inertial uncertainty. Also, since the formation error is less than our desired stopping criteria, r also stabilizes to the desired value instead of continuing to increase linearly with time (or to switch between two constant values). Therefore, we can safely claim that our adaptive and robust passivity-based control frameworks are robust against inertial uncertainty, even that of very high one.

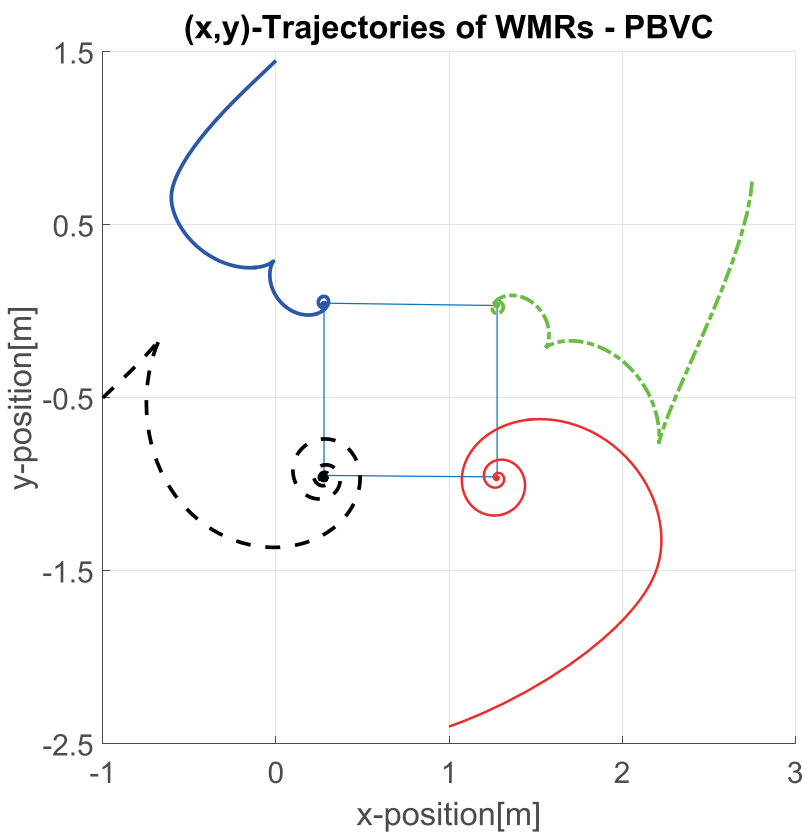

FIGURE 5.2: Simulation of nominal passivity-based time-varying formation stabilization with low inertial uncertainty: Trajectories.

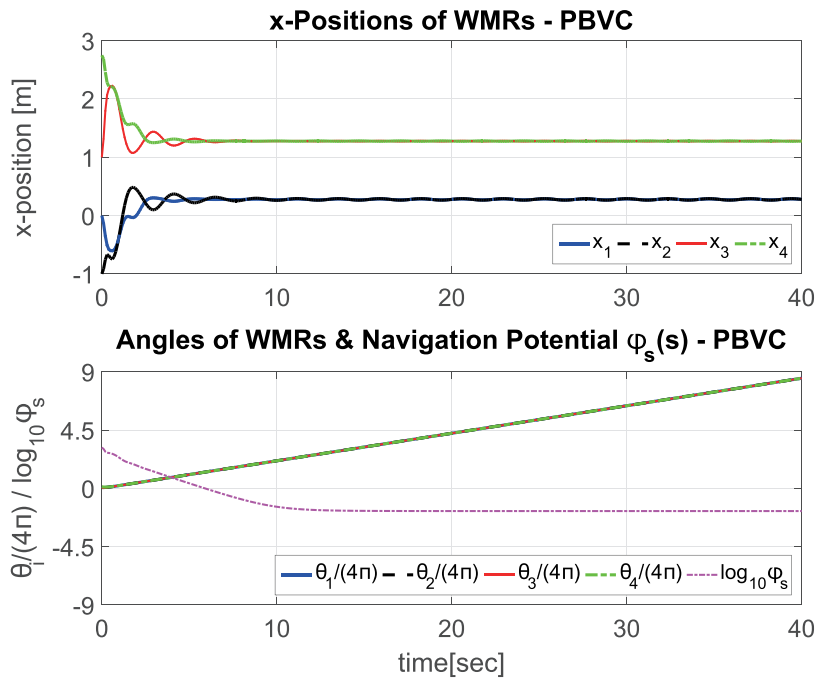

FIGURE 5.3: Simulation of nominal passivity-based time-varying formation stabilization with low inertial uncertainty: Configurations and navigation potential.

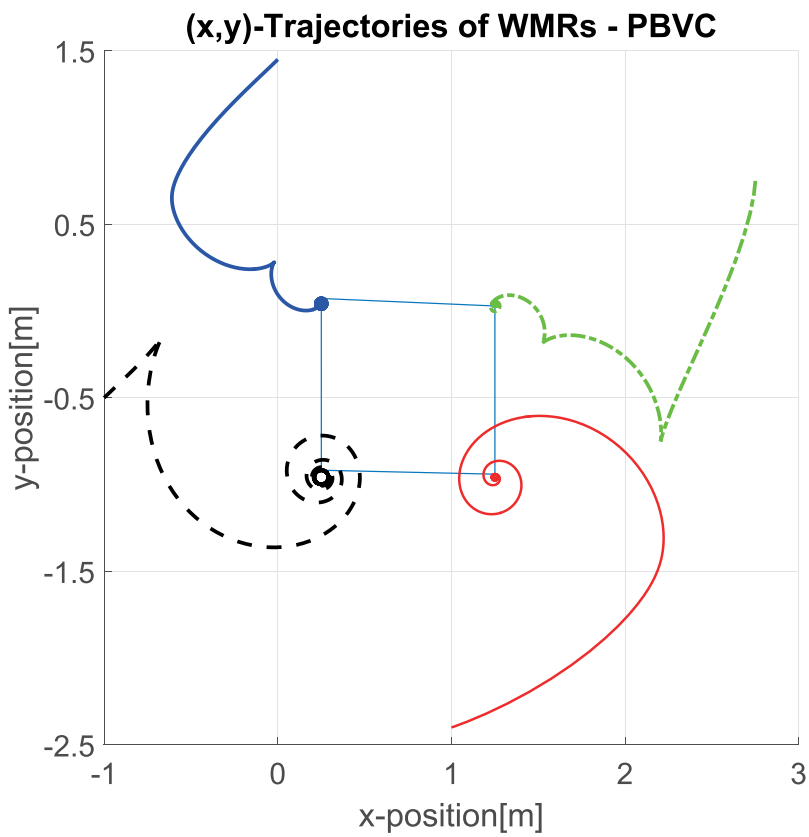

FIGURE 5.4: Simulation of nominal passivity-based time-varying formation stabilization with high inertial uncertainty: Trajectories.

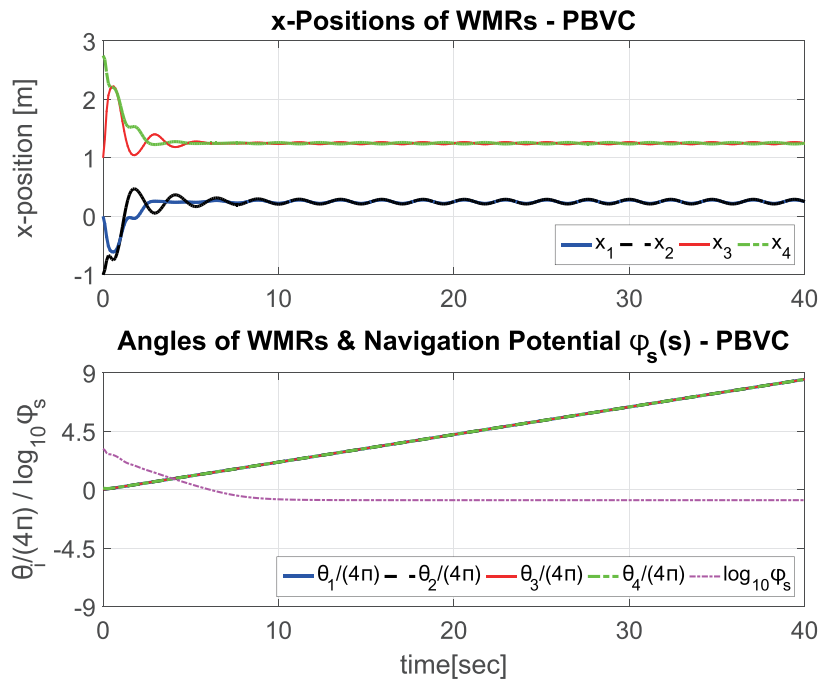

FIGURE 5.5: Simulation of nominal passivity-based time-varying formation stabilization with high inertial uncertainty: Configurations and navigation potential.

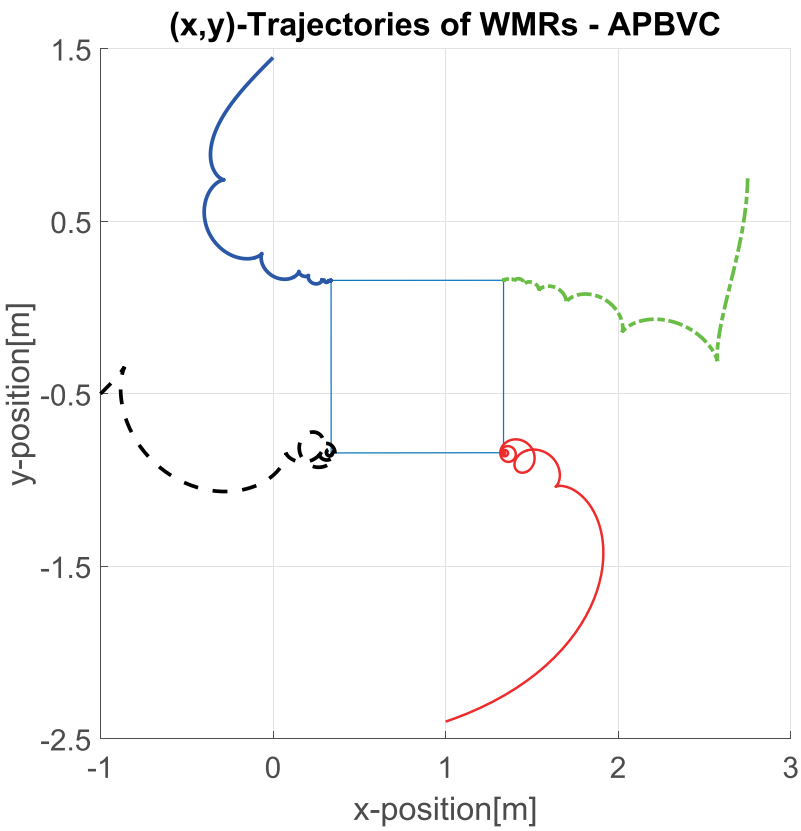

FIGURE 5.6: Simulation of adaptive passivity-based time-varying formation stabilization with low inertial uncertainty: Trajectories.

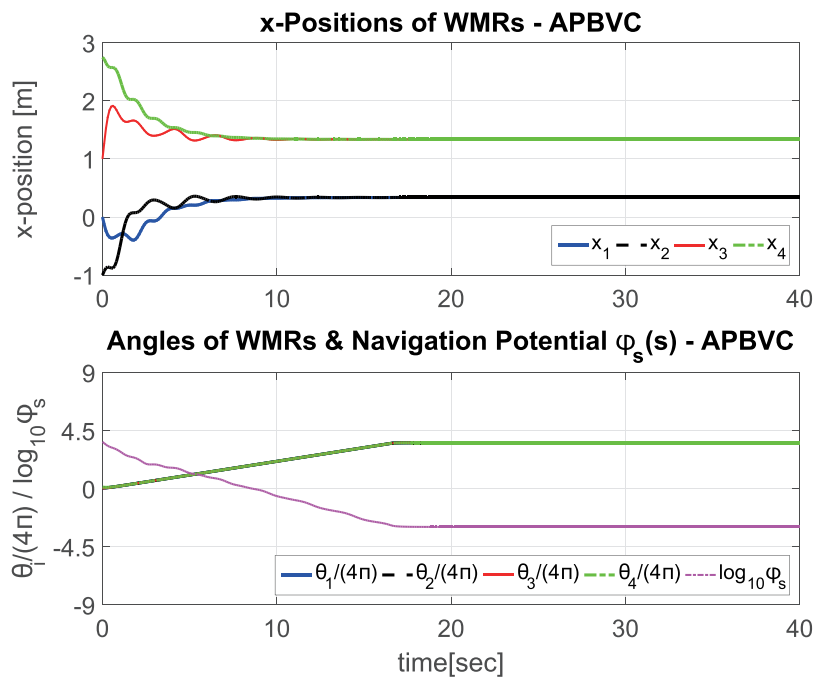

FIGURE 5.7: Simulation of adaptive passivity-based time-varying formation stabilization with low inertial uncertainty: Configurations and navigation potential.

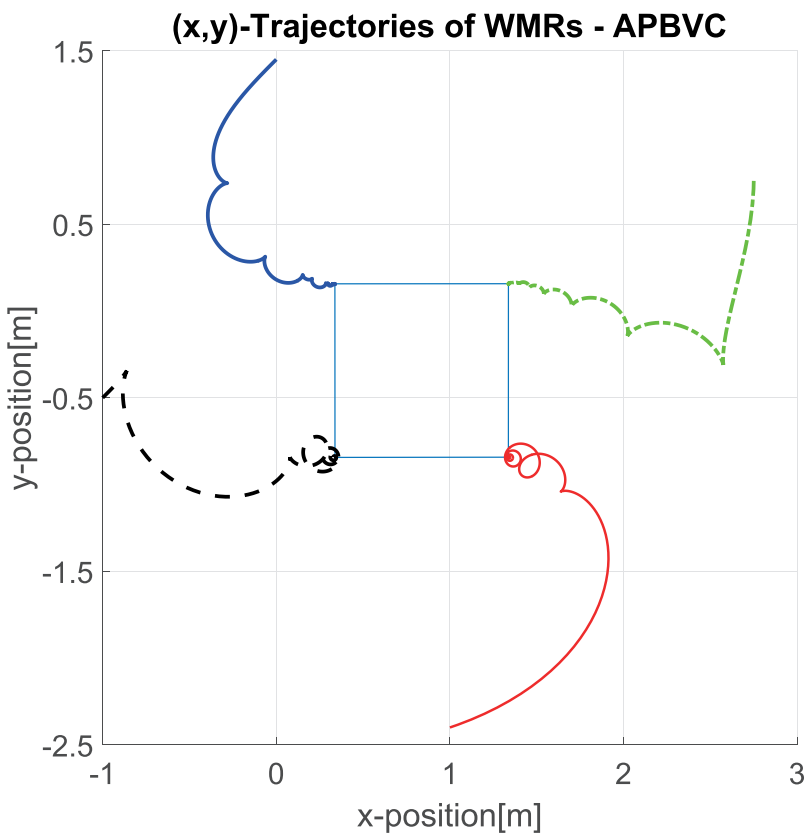

FIGURE 5.8: Simulation of adaptive passivity-based time-varying formation stabilization with high inertial uncertainty: Trajectories.

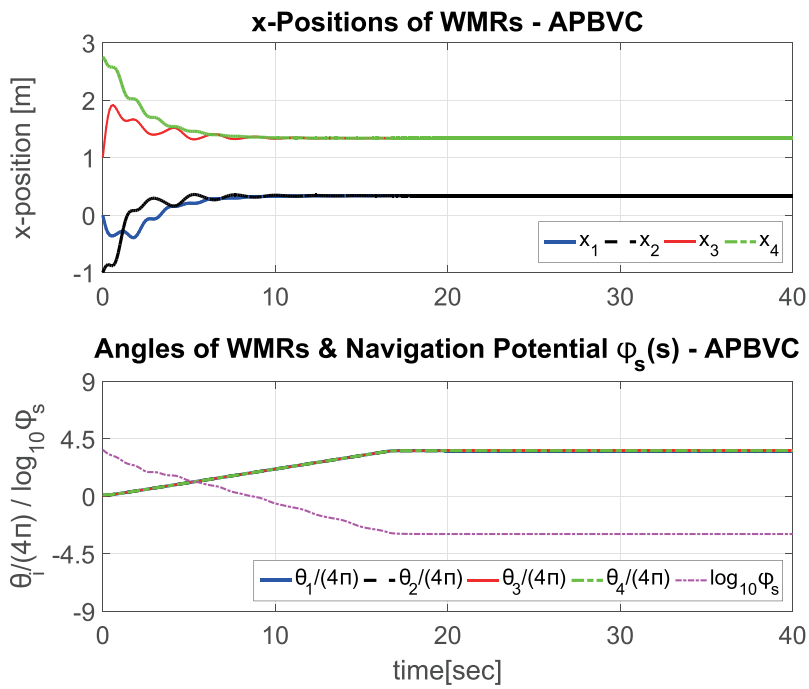

FIGURE 5.9: Simulation of adaptive passivity-based time-varying formation stabilization with high inertial uncertainty: Configurations and navigation potential.

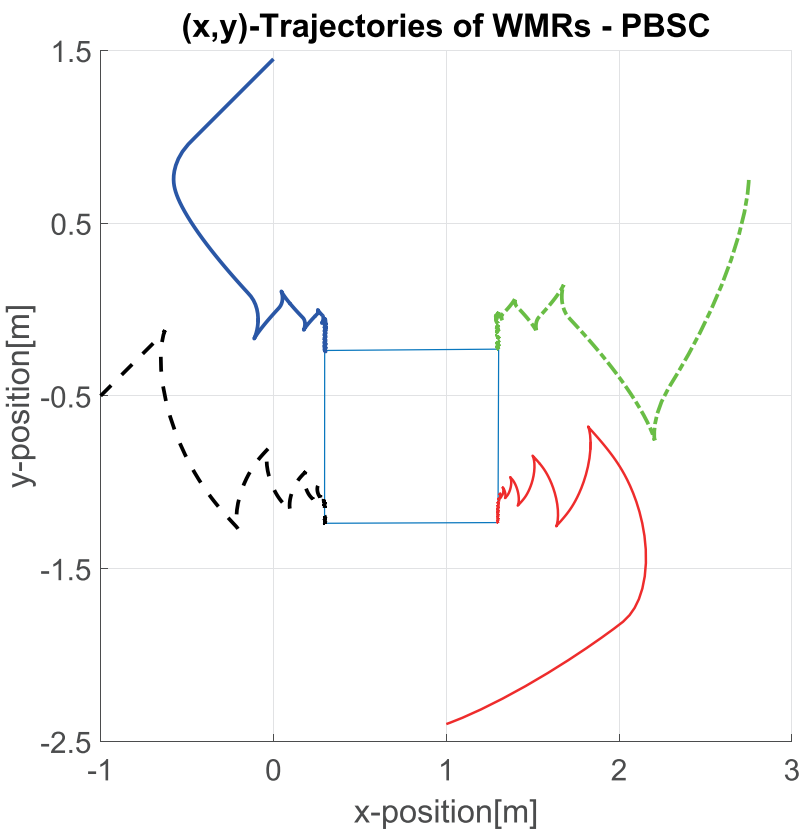

FIGURE 5.10: Simulation of nominal passivity-based switching formation stabilization with low inertial uncertainty: Trajectories.

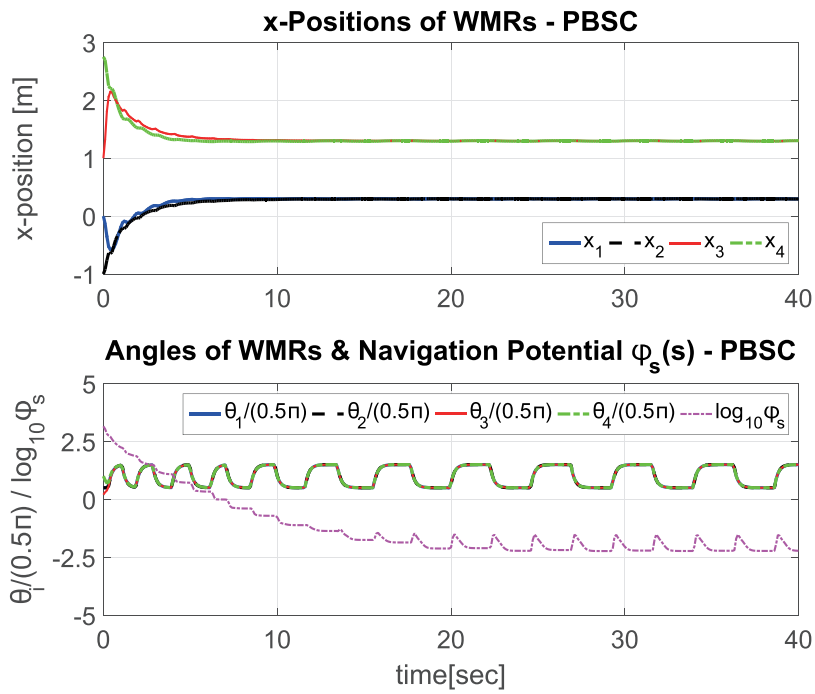

FIGURE 5.11: Simulation of nominal passivity-based switching formation stabilization with low inertial uncertainty: Configurations and navigation potential.

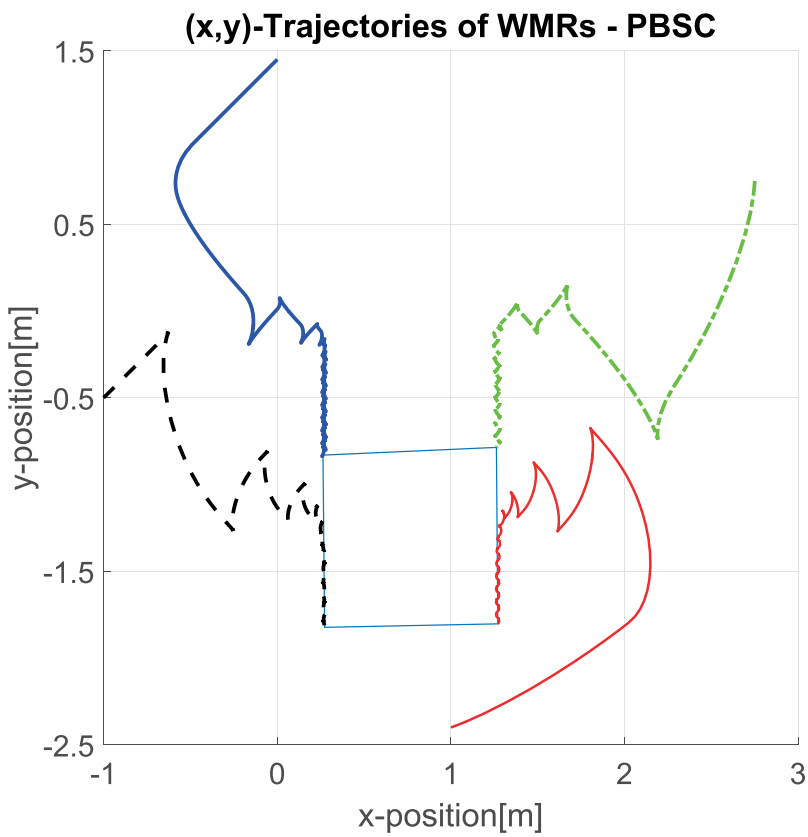

FIGURE 5.12: Simulation of nominal passivity-based switching formation stabilization with high inertial uncertainty: Trajectories.

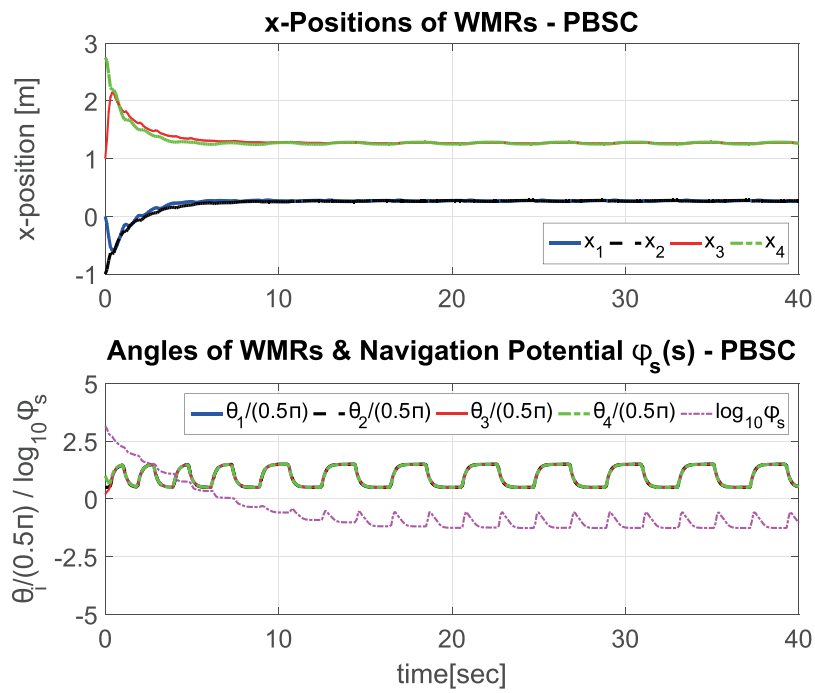

FIGURE 5.13: Simulation of nominal passivity-based switching formation stabilization with high inertial uncertainty: Configurations and navigation potential.

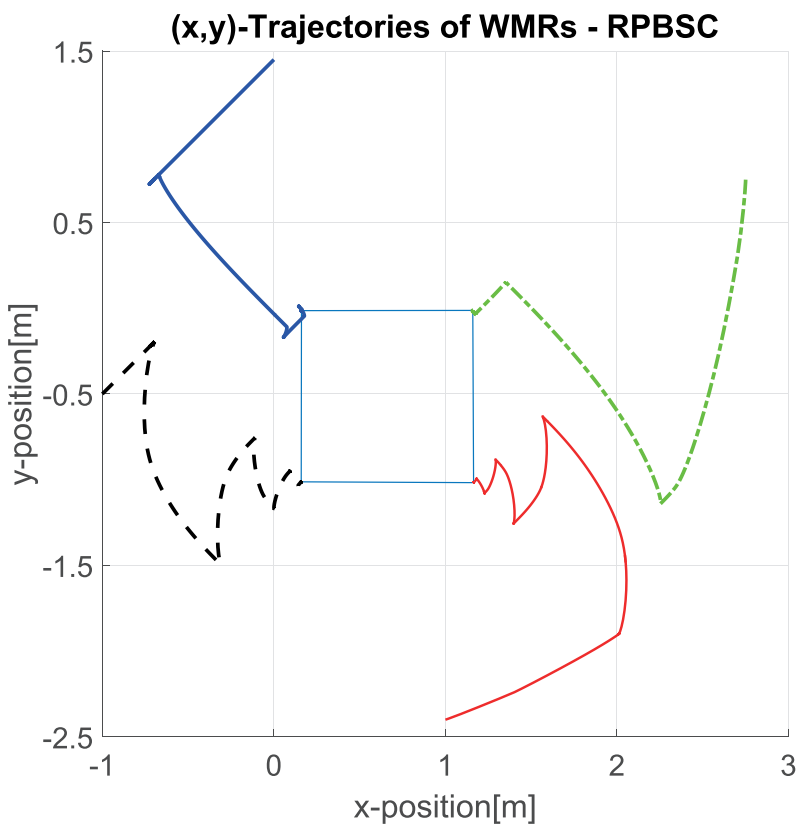

FIGURE 5.14: Simulation of robust passivity-based switching formation stabilization with low inertial uncertainty: Trajectories.

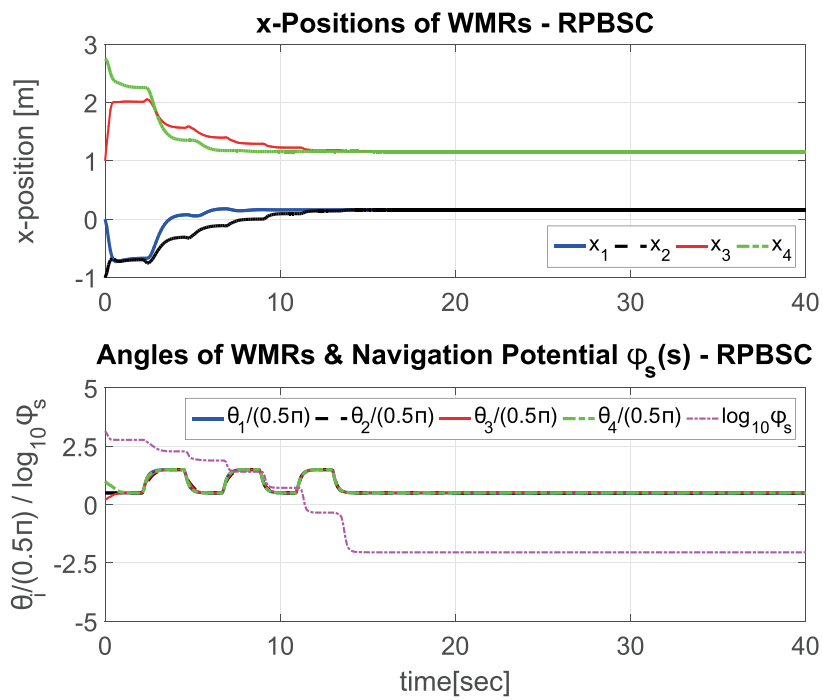

FIGURE 5.15: Simulation of robust passivity-based switching formation stabilization with low inertial uncertainty: Configurations and navigation potential.

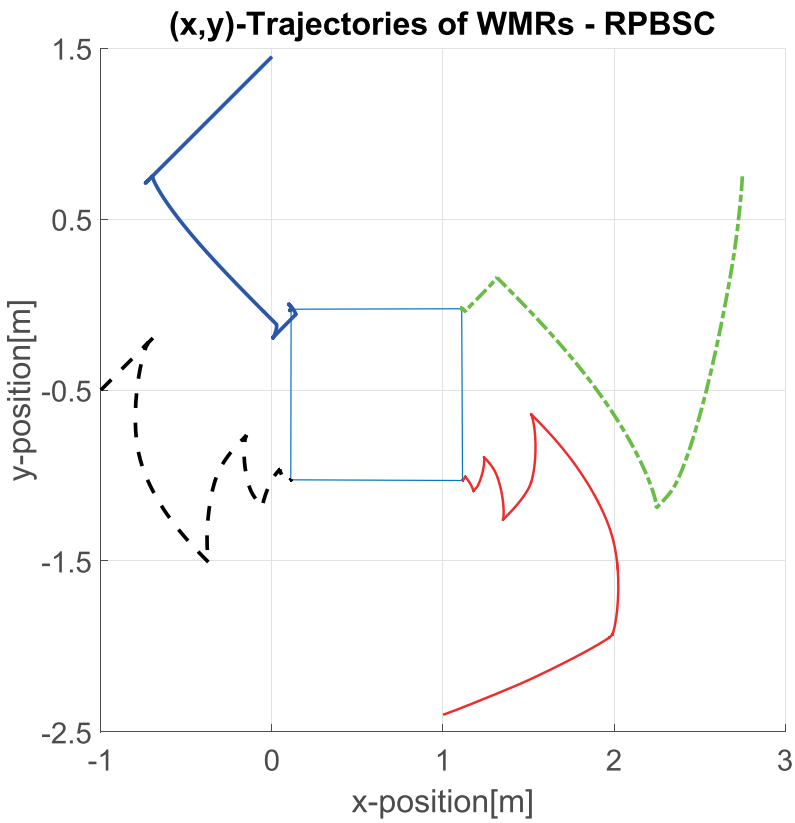

FIGURE 5.16: Simulation of robust passivity-based switching formation stabilization with high inertial uncertainty: Trajectories.

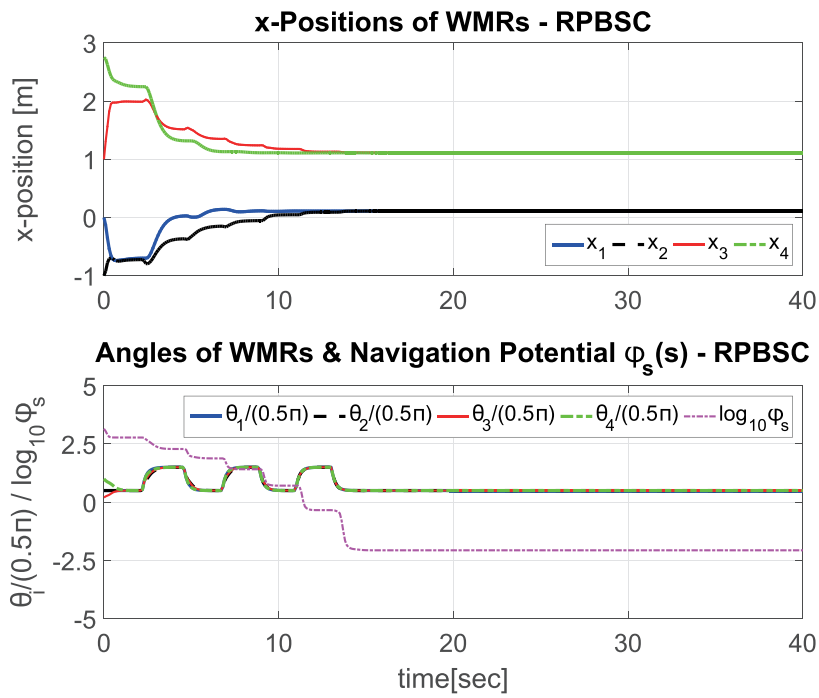

FIGURE 5.17: Simulation of robust passivity-based switching formation stabilization with high inertial uncertainty: Configurations and navigation potential.

5.2 Experiment

FIGURE 5.18: Small and large WMRs with VICON® motion capture system markers used in the experiments.

In addition to simulations, we conduct experiments of multiple WMRs' formation stabilization from Sec. 5.1 to verify our proposed control frameworks for practical applicability. The WMRs used in the experiments are shown in Fig. 5.18. In particular, we use one large WMR as WMR 1 and two small WMRs as WMR 2 and 3 with the measured parameters given as follow: $(m_l, m_s) = (4.74, 3.48)$[kg], $(I_l, I_s) = (11.4 \times 10^{-2}, 3.32 \times 10^{-2})$[kg·m^2], $(c_l, c_s) = (13.5, 10.0)$[cm], $r_l = r_s = 3.25$[cm], and $(d_l, d_s) = (10.0, 5.5)$[cm], where $\star_l$ and $\star_s$ denote the parameters defined in Fig. 5.1 for the large and small WMRs respectively. The WMRs are differential driven by two BLDC motors each. The gearbox reduction ratios are respectively 51:1 and 18:1 for the large and small WMRs. The commands are sent from a ground PC to the WMRs via XBee RF modules. The WMRs' positions and orientations are obtained through VICON® motion capture system at 240[Hz] with their velocities computed from numerical differentiation.

A ring graph G similar to Sec. 5.1 is adopted with the desired formation shape being an isosceles triangle. The stopping criterion is chosen to be $\varphi_s \leq 0.01$, with $k_s = 65$ for the nominal and adaptive passivity-based time-varying control and $k_s = 75$ for the nominal and robust passivity-based switching control. The experimental results are shown in Fig. 5.19 to 5.22 for passivity-based time-varying control (PBVC), Fig. 5.23 to 5.26 for adaptive passivity-based time-varying control (APBVC), Fig. 5.27 to 5.30 for passivity-based switching control (PBSC), and Fig. 5.31 to 5.34 for robust passivity-based switching control (RPBSC).

In general, we can see that the experimental results show similar trend as the simulation results in Sec. 5.1. From Fig. 5.20, 5.28 (low inertial uncertainty) and Fig. 5.22, 5.30 (high inertial uncertainty), we can see that the WMRs' x-positions oscillate w.r.t. the desired set-points, but not being able to converge to them. Similar to Sec. 5.1, since the formation error does not decrease below our desired stopping criterion, r continues to increase linearly with time for PBVC and to switch between two constant values for PBSC.

On the other hand, from Fig. 5.23 to 5.26 for APBVC and Fig. 5.31 to 5.34 for RPBSC, we can see that, instead of oscillating w.r.t. the desired set-points, the WMRs' x-positions converge shortly after about 8[sec] for APBVC and 17[sec] for RPBSC even with high inertial uncertainty. Since the formation error is less than our desired stopping criterion, r also stabilizes instead of continuing to increase linearly with time (or to switch between two constant values). Note that the RPBSC exhibits slower convergence due to the WMRs' stopping at each

switching. This convergence time can be shorten by optimizing the switching action and control gains, e.g. allowing the WMRs to transverse a larger distance D on $\mathcal{S}$ during each switching so that the last line of (4.15) is highly negative, hence reducing the navigation potential $\varphi_s(t)$ more at each switching. Note also that the control gains here are by no means optimal. Optimizing the switching (or time-varying) actions and control gains for better performance will be a topic for future research.

From Fig. 5.19, 5.21 for PBVC, and Fig. 5.27, 5.29 for PBSC, we can see that the WMRs "float" around and cannot converge, yet still maintain the desired isosceles triangle formation to a certain extent. Again, the formation error does not decrease below a certain steady-state error due to the inertial uncertainty, which needs to be compensated by adaptive or sliding-mode actions. With low inertial uncertainty, the Euclidean norms of the oscillating formation error on average are about 3.58[cm] and 3.44[cm] for PBVC and PBSC respectively. These average Euclidean norms are about 4.60[cm] and 4.75[cm] for PBVC and PBSC respectively with high inertial uncertainty. Here, we use the average Euclidean norm of the oscillating formation error instead of the terminal Euclidean norm of the formation error since the WMRs do not stabilize to a final formation. We can then see that these nominal counterparts of our passivity-based control frameworks are relatively robust against low inertial uncertainty, and would likely be sufficient for applications which do not require highly precise control.

On contrary, from Fig. 5.23, 5.25 for APBVC, and Fig. 5.31, 5.33 for RPBSC, the

WMRs converge to the desired formation with its centroid symmetric in SE(2). The formation error's terminal Euclidean norms are 0.96[cm] and 0.89[cm] for APBVC and RPBSC respectively with low inertial uncertainty; and 0.84[cm] and 0.90[cm] respectively with high inertial uncertainty. These values do not vary significantly even when the inertial uncertainty is high. Therefore, we can then claim that our adaptive and robust passivity-based control frameworks are robust against inertial uncertainty, even that of very high one, in addition to other disturbances such as sensor noises, sampling effect, etc.

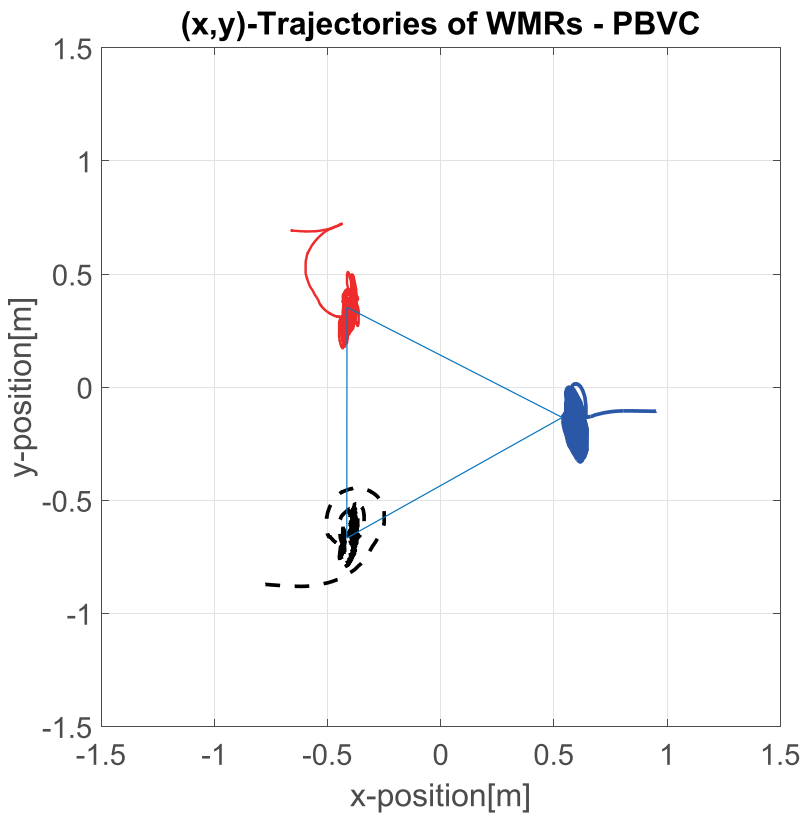

FIGURE 5.19: Experiment of nominal passivity-based time-varying formation stabilization with low inertial uncertainty: Trajectories.

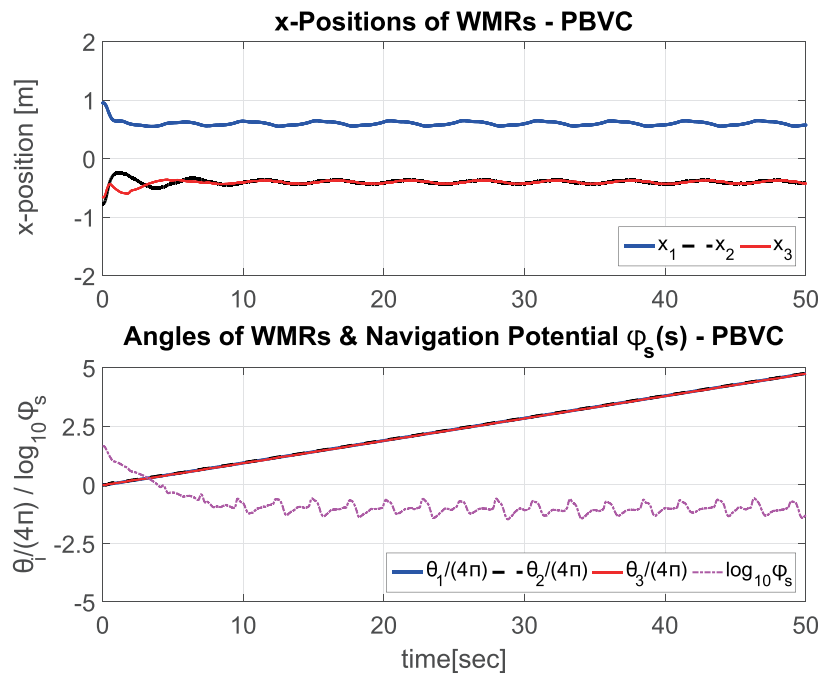

FIGURE 5.20: Experiment of nominal passivity-based time-varying formation stabilization with low inertial uncertainty: Configurations and navigation potential.

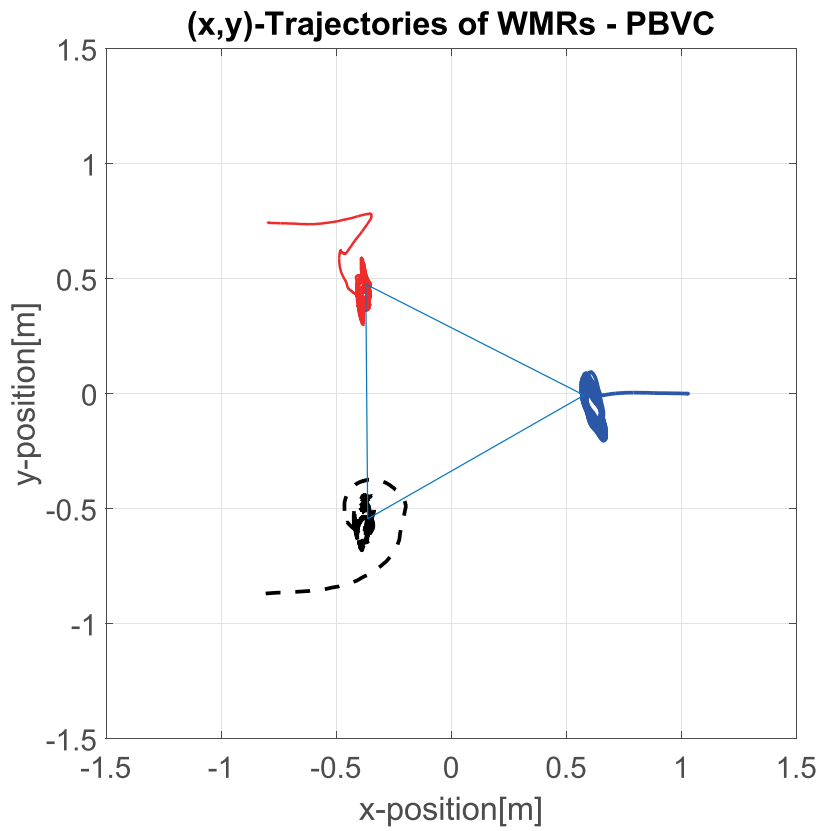

FIGURE 5.21: Experiment of nominal passivity-based time-varying formation stabilization with high inertial uncertainty: Trajectories.

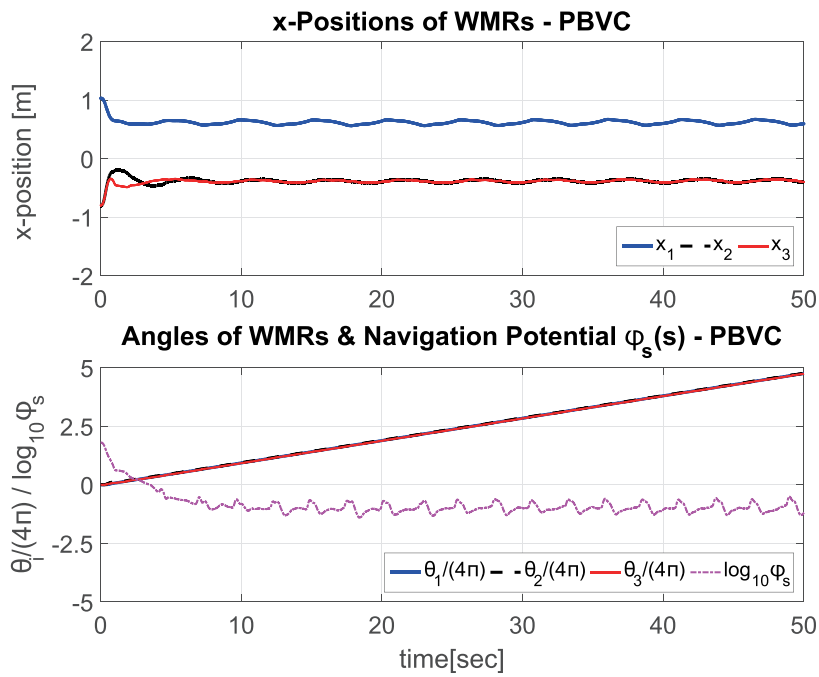

FIGURE 5.22: Experiment of nominal passivity-based time-varying formation stabilization with high inertial uncertainty: Configurations and navigation potential.

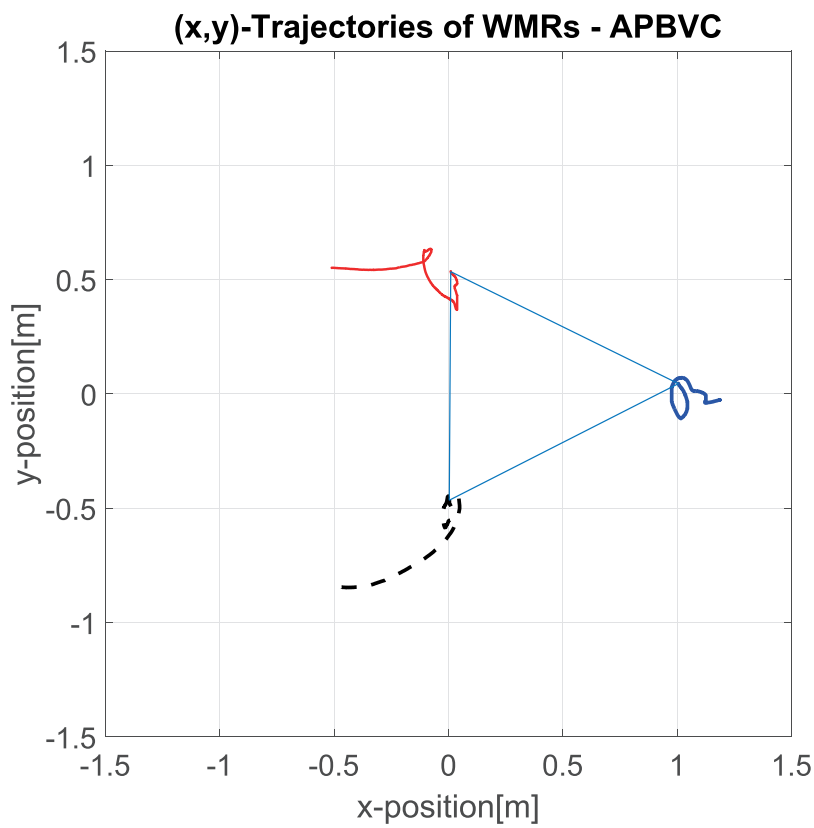

FIGURE 5.23: Experiment of adaptive passivity-based time-varying formation stabilization with low inertial uncertainty: Trajectories.

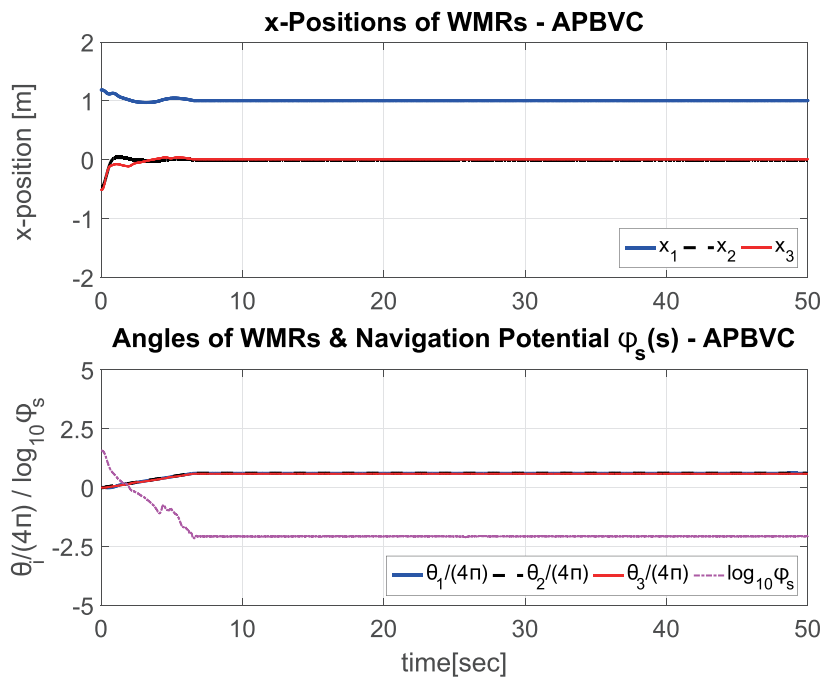

FIGURE 5.24: Experiment of adaptive passivity-based time-varying formation stabilization with low inertial uncertainty: Configurations and navigation potential.

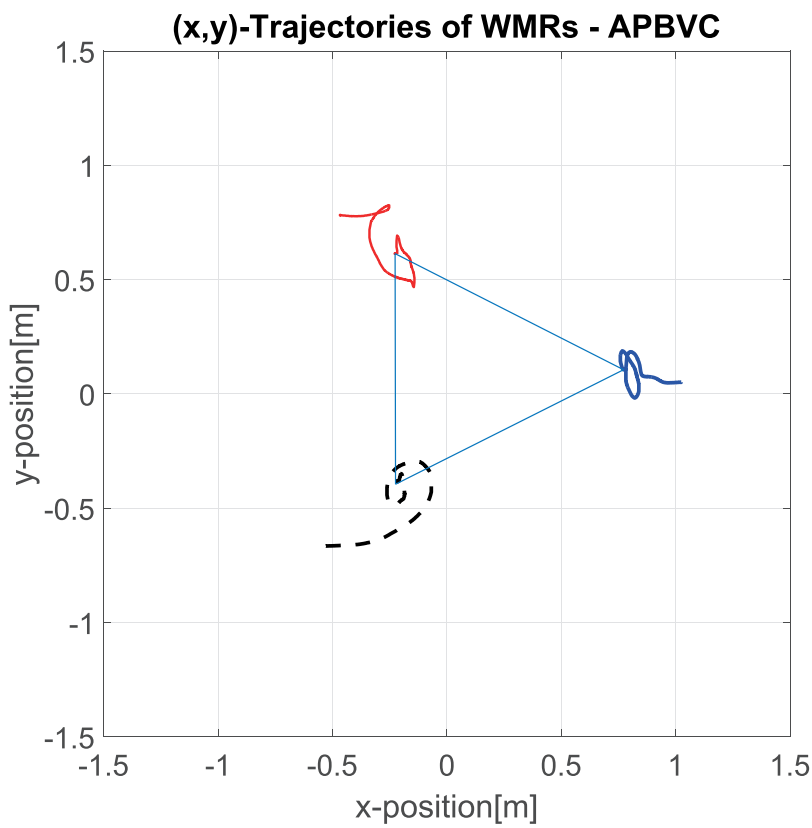

FIGURE 5.25: Experiment of adaptive passivity-based time-varying formation stabilization with high inertial uncertainty: Trajectories.

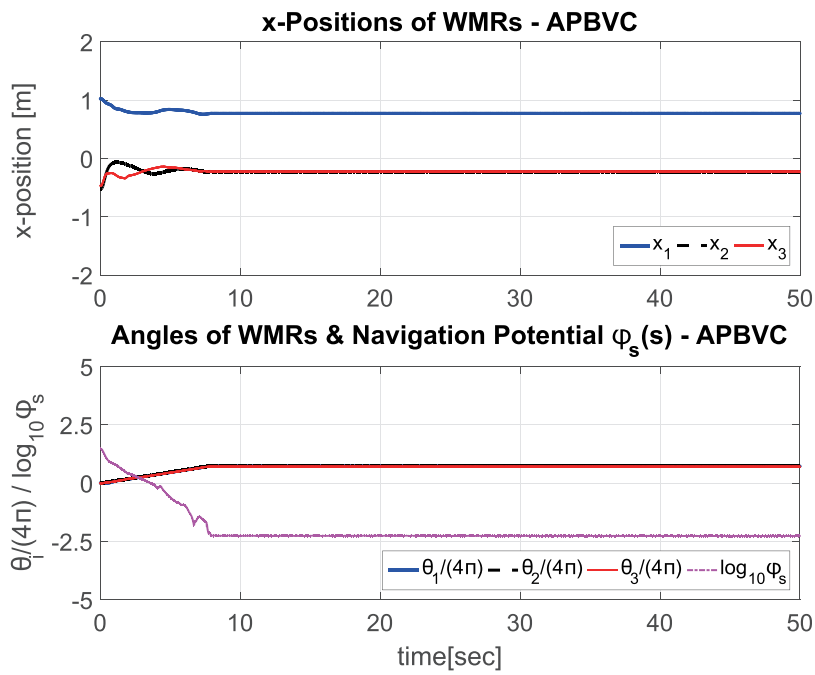

FIGURE 5.26: Experiment of adaptive passivity-based time-varying formation stabilization with high inertial uncertainty: Configurations and navigation potential.

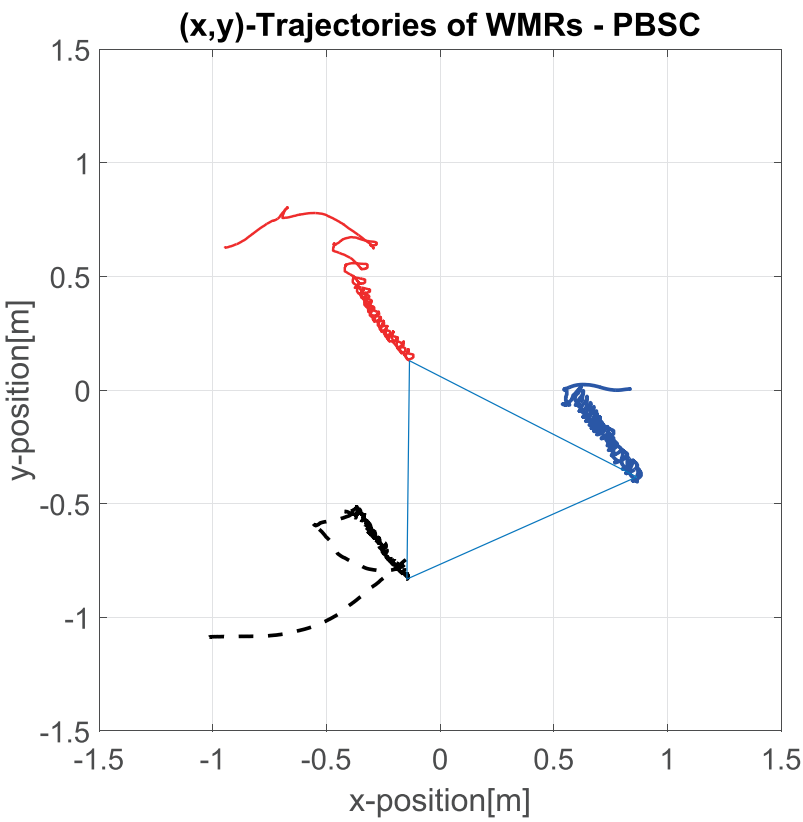

FIGURE 5.27: Experiment of nominal passivity-based switching formation stabilization with low inertial uncertainty: Trajectories.

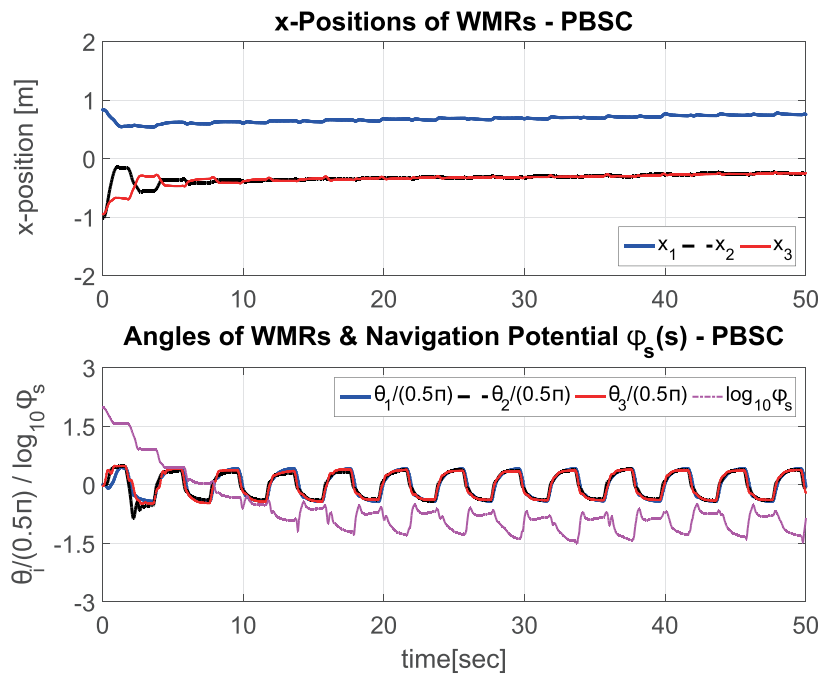

FIGURE 5.28: Experiment of nominal passivity-based switching formation stabilization with low inertial uncertainty: Configurations and navigation potential.

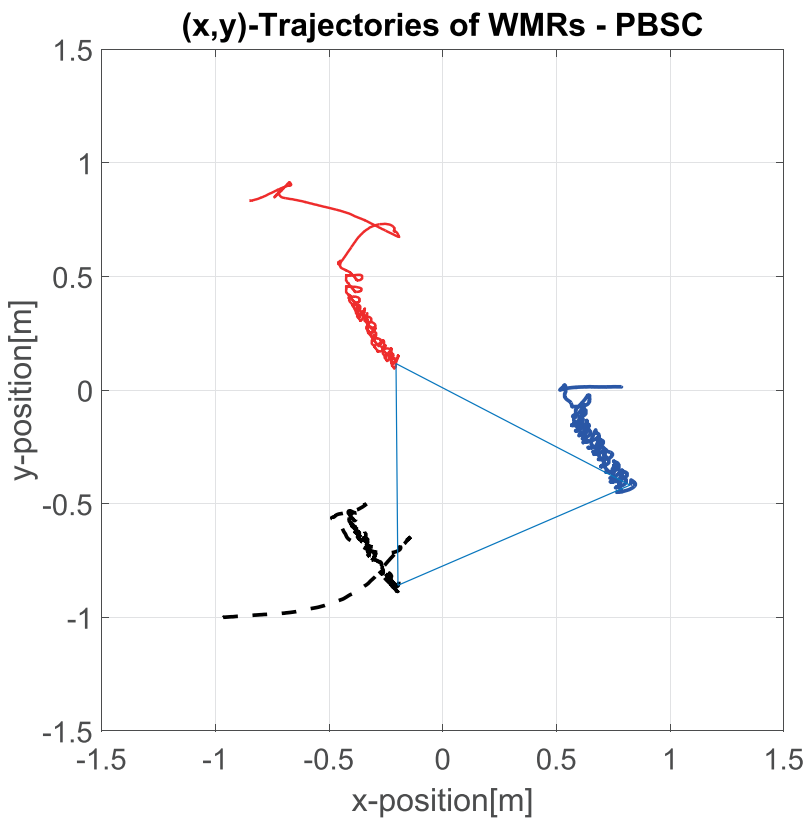

FIGURE 5.29: Experiment of nominal passivity-based switching formation stabilization with high inertial uncertainty: Trajectories.

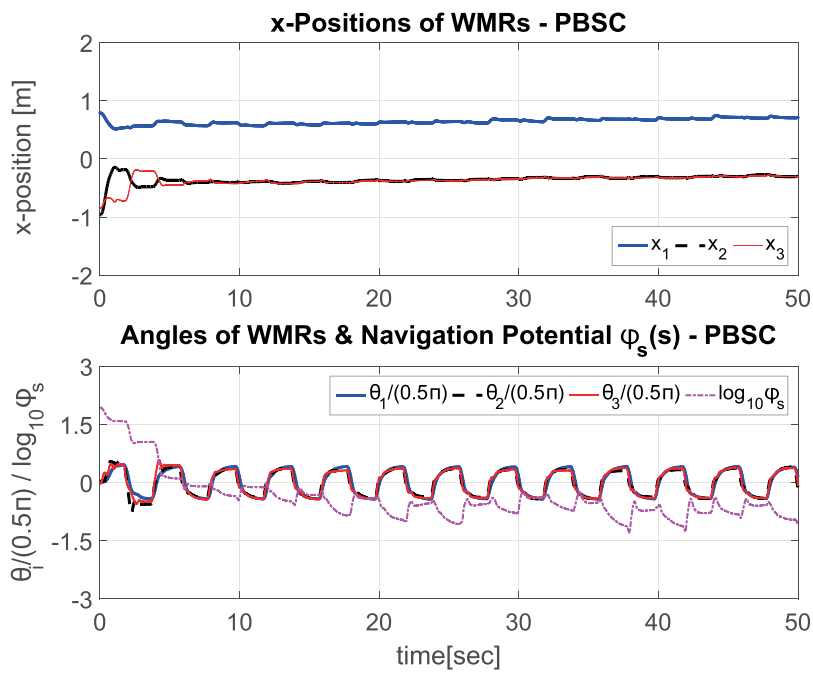

FIGURE 5.30: Experiment of nominal passivity-based switching formation stabilization with high inertial uncertainty: Configurations and navigation potential.

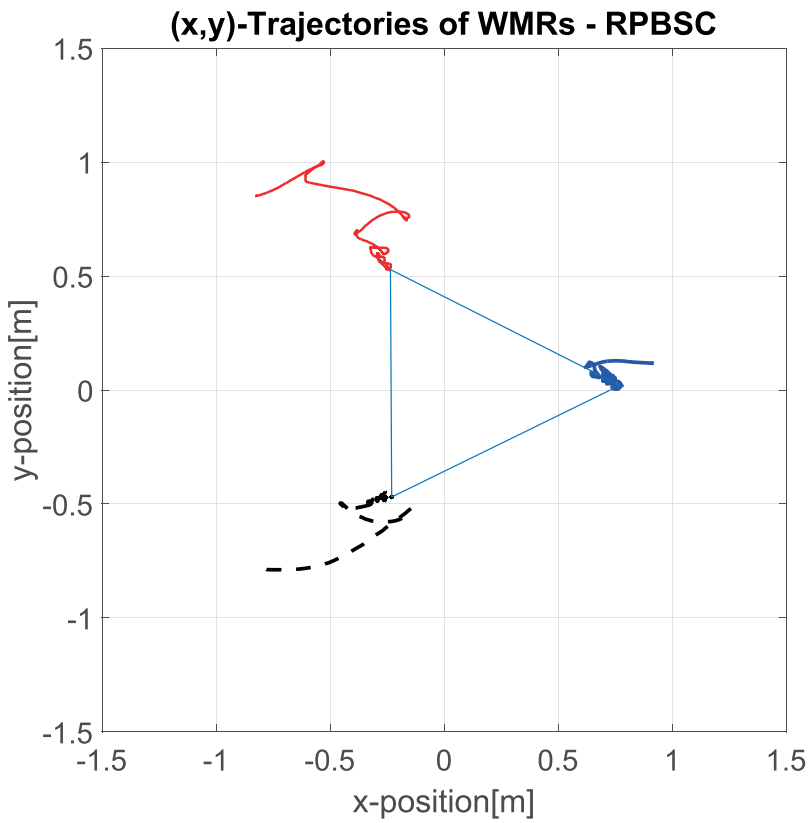

FIGURE 5.31: Experiment of robust passivity-based switching formation stabilization with low inertial uncertainty: Trajectories.

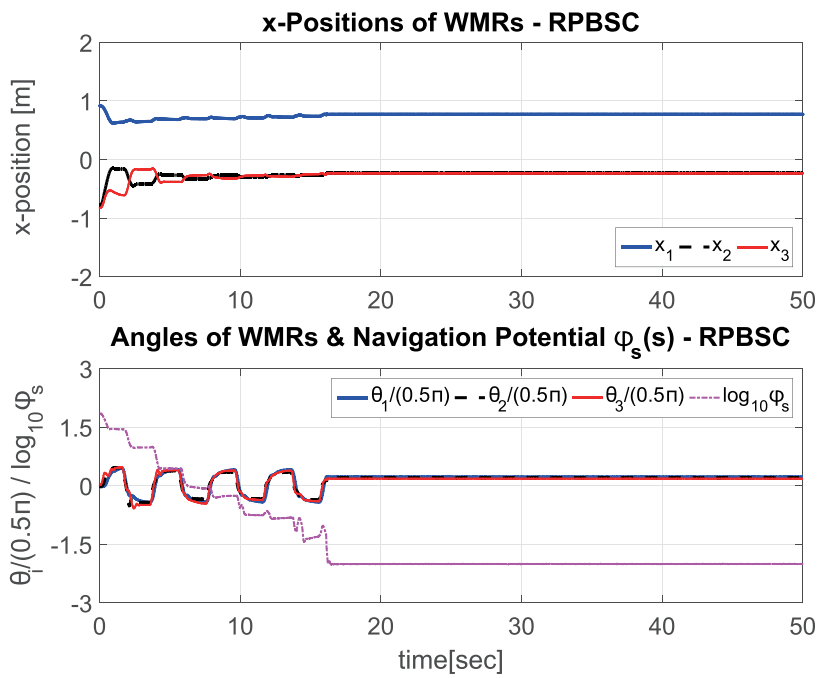

FIGURE 5.32: Experiment of robust passivity-based switching formation stabilization with low inertial uncertainty: Configurations and navigation potential.

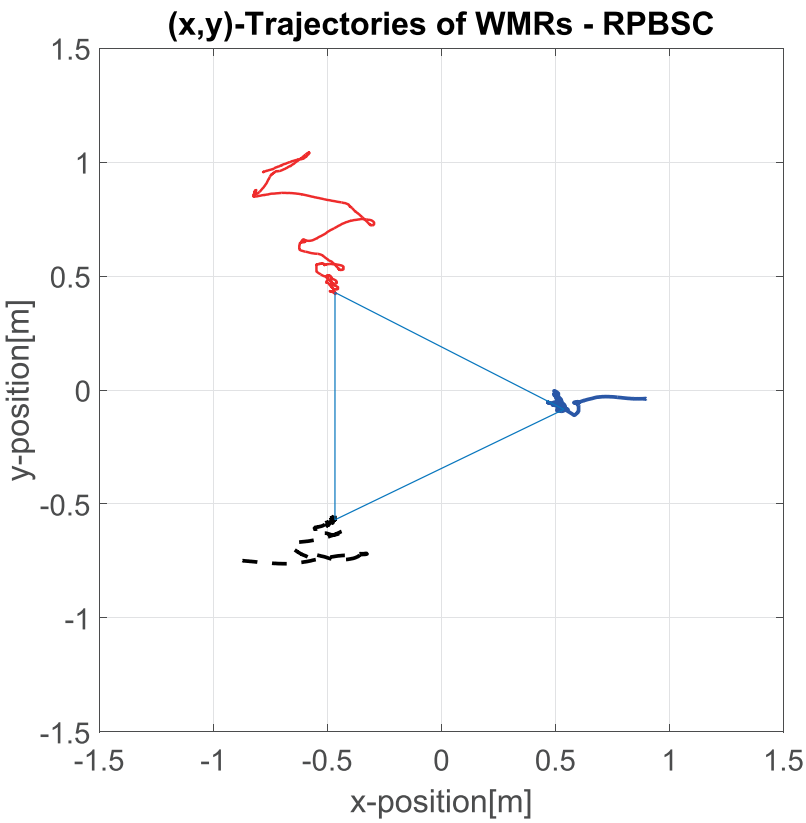

FIGURE 5.33: Experiment of robust passivity-based switching formation stabilization with high inertial uncertainty: Trajectories.

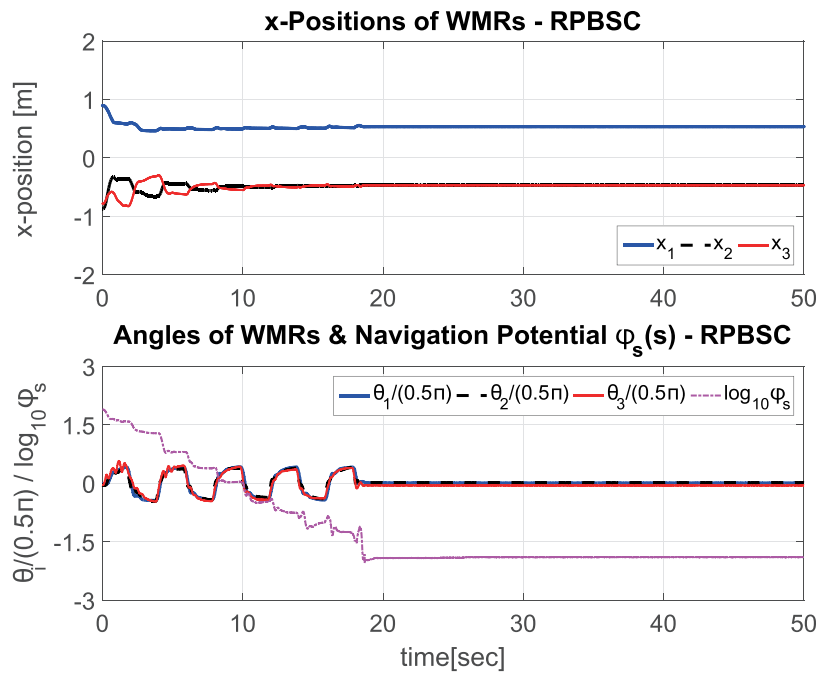

FIGURE 5.34: Experiment of robust passivity-based switching formation stabilization with high inertial uncertainty: Configurations and navigation potential.

Chapter 6

Conclusion and Future Work

6.1 Conclusion

In this thesis, we propose novel passivity-based stabilization control frameworks for a class of nonholonomic mechanical systems with uncertain inertial parameters. Passive configuration decomposition is first applied to configuration-level decompose the system's Lagrange-D'Alembert dynamics into two systems, each inheriting Lagrangian structure and passivity from the original dynamics. Utilizing the nonlinearity and passivity of the decomposed dynamics, we propose adaptive passivity-based time-varying control (APBVC) and robust passivity-based switching control (RPBSC) schemes to achieve stabilization for this certain class

of nonholonomic mechanical systems. These control frameworks adopt the concepts of adaptive control and sliding-mode control respectively to compensate for the inertial uncertainty. Both simulation and experimental results are provided to verify our proposed control frameworks, from which we find that the control frameworks are robust against inertial uncertainty, even that of very high one. We also find that the nominal counterparts of our control frameworks are fairly robust for the cases with low inertial uncertainty.

6.2 Future Work

One of the future research topics would be the optimization of time-varying and switching control actions. More specifically, we could optimize such actions based on electrical power consumption, which results can be applied to the nonholonomic robots for logistic applications such as Fetch Robotics and Amazon Robotics. These robots usually run 24 hours per day, hence electrical power consumption would be a critical factor to be considered. We could also optimize the control actions w.r.t. convergence time for faster convergence.

Besides that, other possible future research topics include: 1) extension of our control frameworks to various control objectives, e.g. trajectory tracking, obstacle avoidance; 2) derivation of the conditions for parameter convergence for adaptive passivity-based time-varying control; 3) incorporation of underactuation in $\mathcal{D}$;

and 4) extensive experimental comparisons of our control frameworks against other control approaches.

Bibliography

[1] K. Y. Lui, H. Cho, C. Ha, and D. J. Lee. First person view semi-autonomous teleoperation of cooperative wmrs with visuo-haptic feedback. *International Journal of Robotics Research, submitted*, 2016.

[2] M. W. Spong, S. Hutchinson, and M. Vidyasaga. *Robot modeling and control*. John Wiley & Sons, Hoboken, NJ, 2006.

[3] I. Fantoni, R. Lozano, and M. W. Spong. Energy based control of the pendubot. *IEEE Transactions on Automatic Control*, 45(4):725–729, 2000.

[4] R. Ortega, M. W. Spong, and F. Gómez-Estern. Stabilization of a class of underactuated mechanical systems via interconnection and damping assignment. *IEEE Transactions on Automatic Control*, 47(8):1218–1233, 2002.

[5] B. Brogliato, R. Ortega, and R. Lozano. Global tracking controllers for flexible-joint manipulators: a comparative study. *Automatica*, 31(7):941–956, 1995.

[6] A. Albu-Schäffer, C. Ott, and G. Hirzinger. A unified passivity-based control framework for position, torque and impedance control of flexible joint robots. *International Journal of Robotics Research*, 26(1):23–39, 2007.

[7] J-J. E. Slotine and W. Li. On the adaptive control of robot manipulators. *International Journal of Robotics Research*, 6(3):49–59, 1987.

[8] P. Y. Li and R. Horowitz. Passive velocity field control: Part 1. geometry and robustness. *IEEE Transactions on Automatic Control*, 46(9):1346–1359, 2001.

[9] S. Stramigioli. *Modelling and IPC Control of Interactive Mechanical Systems: a Coordinate-free Approach*. Springer.

[10] S. P. Buerger and N. Hogan. Complementary stability and loop shaping for improved human-robot interaction. *IEEE Transactions on Robotics*, 23(2): 232–244, 2007.

[11] M. W. Spong, J. K. Holm, and D. J. Lee. Passivity-based control of bipedal locomotion. *IEEE Robotics & Automation Magazine*, 14(2):30–40, 2007.

[12] D. J. Lee and P. Y. Li. Passive bilateral control and tool dynamics rendering for nonlinear mechanical teleoperators. *IEEE Transactions on Robotics*, 21 (5):936–951, 2005.

[13] D. J. Lee and M. W. Spong. Passive bilateral teleoperation with constant time delay. *IEEE Transactions on Robotics*, 22(2):269–281, 2006.

[14] C. Canudas de Wit and O. J. Sordalen. Exponential stabilization of mobile robots with nonholonomic constraints. *IEEE Transactions on Automatic Control*, 37(11):1791–1797, 1992.

[15] A. Bloch, M. Reyhanoglu, and N. H. McClamroch. Control and stabilization of nonholonomic dynamic systems. *IEEE Transactions on Automatic Control*, 37(11):1746–1757, 1992.

[16] I. Kolmanovsky and N. H. McClamroch. Developments in nonholonomic control problems. *IEEE Control Systems Magazine*, 15(6):20–36, 1995.

[17] M. Aicardi, G. Casalino, A. Bicchi, and A. Balestrino. Closed-loop steering of unicycle-like vehicles via lyapunov techniques. *IEEE Robotics & Automation Magazine*, 2(1):27–35, 1995.

[18] I. Kolmanovsky, M. Reyhanoglu, and N. H. McClamroch. Switched mode feedback control laws for nonholonomic systems in extended power form. *Systems & Control Letters*, 27(1):29–36, 1996.

[19] R. T. M'Closkey and R. M. Murray. Exponential stabilization of driftless nonlinear control systems using homogeneous feedback. *IEEE Transactions on Automatic Control*, 42(5):614–628, 1997.

[20] J. P. Hespanha, D. Liberzon, and A. S. Morse. Logic-based switching control of a nonholonomic system with parametric modeling uncertainty. *Systems & Control Letters*, 38(3):167–177, 1999.

[21] Z.-P. Jiang, E. Lefeber, and H. Nijmeijer. Saturated stabilization and tracking of a nonholonomic mobile robot. *Systems & Control Letters*, 42(5): 327–332, 2001.

[22] P. Morin and C. Samson. Practical stabilization of driftless systems on lie groups: the transverse function approach. *IEEE Transactions on Automatic Control*, 48(9):1496–1508, 2003.

[23] D. J. Lee. Passive decomposition and control of nonholonomic mechanical systems. *IEEE Transactions on Robotics*, 26(6):978–992, 2010. ISSN 1552-3098. doi: 10.1109/TRO.2010.2082430.

[24] K. Fujimoto and T. Sugie. Stabilization of hamiltonian systems with nonholonomic constraints based on time-varying generalized canonical transformation. *Systems & Control Letters*, 44(4):309–319, 2001.

[25] V. Duindam and S. Stramigioli. Energy-based model-reduction of nonholonomic mechanical systems. In *Proceedings of the IEEE Int'l Conf. on Robotics & Automation, pages 4584–4589, 2004.*

[26] J. Ostrowski and J. Burdick. The geometric mechanics of undulatory robotic locomotion. *International Journal of Robotics Research*, 17(7):683–701, 1998.

[27] J. P. Ostrowski, J. P. Desai, and V. Kumar. Optimal gait selection for nonholonomic locomotion systems. *International Journal of Robotics Research*, 19(3):225–237, 2000.

[28] J. Ostrowski. Steering for a class of dynamic nonholonomic systems. *IEEE Transactions on Automatic Control*, 45(8):1492–1498, 2000.

[29] A. D. Lewis. Simple mechanical control systems with constraints. *IEEE Transactions on Automatic Control*, 45(8):1420–1436, 2000.

[30] F. Bullo and K. Lynch. Kinematic controllability for decoupled trajectory planning in underactuated mechanical systems. *IEEE Transactions on Robotics & Automation*, 17(4):402–412, 2001.

[31] Z-P. Jiang. Robust exponential regulation of nonholonomic systems with uncertainties. *Automatica*, 36(2):189–209, 2000.

[32] M. Oya, C-Y. Su, and R. Katoh. Robust adaptive motion/force tracking control of uncertain nonholonomic mechanical systems. *IEEE Transactions on Robotics and Automation*, 19(1):175–181, 2003.

[33] W. Dong and K-D. Kuhnert. Robust adaptive control of nonholonomic mobile robot with parameter and nonparameter uncertainties. *IEEE Transactions on Robotics*, 21(2):261–266, 2005.

[34] Z. Li, S. S. Ge, M. Adams, and W. S. Wijesoma. Robust adaptive control of uncertain force/motion constrained nonholonomic mobile manipulators. *Automatica*, 44(3):776–784, 2008.

[35] S. S. Ge, J. Wang, T. H. Lee, and G. Y. Zhou. Adaptive robust stabilization of dynamic nonholonomic chained systems. *Journal of Robotic Systems*, 18 (3):119–133, 2001.

[36] J-M. Yang and J-H. Kim. Sliding mode control for trajectory tracking of nonholonomic wheeled mobile robots. *IEEE Transactions on Robotics and Automation*, 15(3):578–587, 1999.

[37] D. J. Lee, C. Kim, and H-N. Nguyen. Passive configuration decomposition and passivity-based control of nonholonomic mechanical systems. *IEEE Transactions on Robotics, revised and resubmitted*, 2015.

[38] H. Yang and D. J. Lee. Cooperative grasping control of multiple mobile manipulators with obstacle avoidance. In *Proc. IEEE Int'l Conference on Robotics & Automation*, pages 828–833, 2013.

[39] J. P. Ostrowski. Computing reduced equations for robotic systems with constraints and symmetries. *IEEE Transactions on Robotics and Automation*, 15(1):111–123, 1999.

[40] A. M. Bloch. *Nonholonomic mechanics and control*. Springer, New York, NY, 2003. ISBN 9780387955353.

[41] D. J. Lee. Passivity-based switching control for stabilization of wheeled mobile robots. In *Proc. Robotics: Science & Systems*, pages 70–77, 2007.

[42] A. M. Bloch, P. S. Krishnaprasad, J. E. Marsden, and R. M. Murray. Nonholonomic mechanical systems with symmetry. *Archive for Rational Mechanics and Analysis*, 136(1):21–99, 1996.

[43] O. Khatib. Real-time obstacle avoidance for manipulators and mobile robots. *International Journal of Robotics Research*, 5(1):90–98, 1986.

[44] S. Sastry. *Nonlinear systems: analysis, stability and control*. Springer, New York, NY, 1999.

[45] W. Ren and R. Beard. Consensus seeking in multiagent systems under dynamically changing interaction topologies. *IEEE Transactions on Automatic Control*, 50(5):655–661, 2005.

요약

본 논문에서는 불확실한 관성정보를 가진 일군의 동적 논홀로노믹 기계시스템의 수동성기반 적응 및 강건 안정화 제어기법에 대해서 기술한다. 우선, 논홀로노믹 기계시스템의 동역학을 configuration-level에서 두 개의 시스템으로 분할하기 위하여 passive configuration decomposition 기법을 적용한다. 분할된 두 개의 시스템은 독립적으로 변화할 뿐 아니라 원래의 동역학이 가지는 Lagrangian 구조와 수동성을 유지하는 특성을 가진다. 불확실한 관성정보를 가진 논홀로노믹 기계시스템의 안정화 제어를 위하여 분할 동역학의 비선형성과 수동성을 이용함과 동시에 적응제어기법 및 sliding-mode 제어기법의 개념을 차용하고, 이를 통하여 Adaptive Passivity-Based Time-Varying Control (APBVC, 수동성기반 적응 시변제어)와 Robust Passivity-Based Switching Control (RPBSC, 수동성기반 강건 스위칭제어) 제어기법을 제시한다. 마지막으로 시뮬레이션과 실험 결과를 통해 본 논문에서 제시된 제어기법을 검증하였고 그 결과를 제시하였다.

주요어: 논홀로노믹 구속, 불확실한 관성정보, 적응제어, 강건제어
학번: *2014-22194*